Novel *Fusarium* mutualists of two *Euwallacea* species infesting *Acacia crassicarpa* in Indonesia

Kira M. T. Lynn[a], Michael J. Wingfield[a], Alvaro Durán[b], Leonardo S. S. Oliveira[b], Z. Wilhelm de Beer[a], and Irene Barnes[a,*]

[a]Department of Biochemistry, Genetics and Microbiology, Forestry and Agricultural Biotechnology Institute, University of Pretoria, Private Bag X20, Pretoria, 0028, South Africa;
[b]Plant Health Program, Research and Development, Asia Pacific Resources International Holdings Ltd., Pangkalan Kerinci 28300, Riau, Indonesia

*CONTACT: Irene Barnes. Email: irene.barnes@fabi.up.ac.za

ABSTRACT

Several species in the *Euwallacea fornicatus* complex have emerged as important pests of woody plants globally, particularly in habitats where they are invasive aliens. These beetles live in obligate symbioses with fungi in the genus *Fusarium*. In this study, we identified *Euwallacea* spp. and their fungal mutualists that have emerged as pests of planted *Acacia crassicarpa* in Riau, Indonesia. Morphological identification and phylogenetic analyses of the mitochondrial cytochrome oxidase *c* subunit I (*COI*) gene confirmed that *E. similis* and *E. perbrevis* are the most abundant beetles infesting these trees. Multilocus phylogenetic analyses of their fungal mutualists revealed their nonspecific association with six *Fusarium* species. These included *F. rekanum* and five novel *Fusarium* mutualists within the *Fusarium solani* species complex (FSSC), four of which reside in the Ambrosia *Fusarium* Clade (AFC). These new species are described here as *F. akasia, F. awan, F. mekan, F. variasi*, and *F. warna*.

Keywords: Ambrosia beetles; Ambrosia *Fusarium* Clade (AFC); *Euwallacea* symbiosis; *Fusarium*; 5 new taxa

INTRODUCTION

Ambrosia beetles (Coleoptera: Curculionidae: Scolytinae) are wood-boring insects that have a primary nutritional association with fungal mutualists (Francke-Grosmann 1967; Hulcr and Stelinski 2017; Vega and Biedermann 2020). Interest in ambrosia beetles along with their coevolved fungal mutualists has increased substantially in recent years (Carrillo et al. 2019; Hulcr et al. 2020; Mayers et al. 2020). This arises from the numerous new outbreaks of these insects and their fungal mutualists in natural forest ecosystems as well as in urban and agricultural environments, across geographically diverse locations (Hulcr and Dunn 2011; Ploetz et al. 2013; O'Donnell et al. 2016). Although ambrosia beetle infestations do not normally result in significant economic impacts, several species such as those in *Euwallacea, Xylosandrus*, and *Xyleborus* have become significant pests, particularly in areas where they have become invasive (Fraedrich et al. 2015; Hughes et al. 2017; Hulcr and Stelinski 2017).

Ambrosia beetles rely on fungal mutualists as an obligate food source, storing and transporting these microbial mutualists within specialized organs known as mycangia (Francke-Grosmann 1967). Ambrosia beetles can be associated with a variety of fungal species, but the fungal mutualists found within their mycangia are distinct and defined as ambrosia fungi (Mayers et al. 2020). Ambrosia fungi are a diverse array of fungi present within the Ophiostomatales, Hypocreales, and Microscales (Mayers et al. 2020). They are morphologically adapted to the mycangium type of their beetle counterparts and appear to no-longer be able to disperse or survive independently (Mayers et al. 2020). By successfully cultivating these nutritional mutualists, ambrosia beetles are able to survive and breed in the nutritionally poor xylem tissue of their infested plant hosts (Beaver 1989; Harrington 2005).

Fungi associated with ambrosia beetles are typically not plant pathogens and rather act as benign nutritional mutualists in their association with their coevolved beetle hosts (Ploetz et al. 2013; Hulcr and Stelinski 2017). However, in some cases, they can become aggressive tree pathogens (Norris and Baker 1968; Bumrungsri et al. 2008; Fraedrich et al. 2008; Hulcr and Dunn 2011). For example, the invasive ambrosia beetles *Euwallacea fornicatus* and *Euwallacea kuroshio* are responsible for spreading the disease known as *Fusarium* dieback (FD) in parts of California and Florida (Carrillo et al. 2020). This disease poses a serious threat to the local avocado industry, as well as to urban landscapes (Eatough Jones and Paine 2017; Stouthamer et al. 2017). The disease is caused by the complex of fungi mutualistically associated with these two beetle species, mainly *Fusarium euwallaceae* and *Fusarium kuroshium* (Freeman et al. 2013, 2016; Na et al. 2018). Neither of these two ambrosia beetles have been reported as pests in their native environments, presumably due to the coevolution between their microbial mutualist(s) and the surrounding native flora (Stouthamer et al. 2017; Paap et al. 2018). Likewise, *Euwallacea perbrevis* has become an invasive pest on avocado trees in Florida (USA) after its accidental introduction into that region (Carrillo et al. 2016). However, *Euwallacea perbrevis* together with its symbionts, *Fusarium ambrosium* and *Fusarium rekanum*, has been reported as a pest in its native range, but only on non-native trees such as tea (*Camellia sinensis*) in India and Sri Lanka (Danthanarayana 1968), and recently on *Acacia crassicarpa* in Indonesia (Lynn et al. 2020).

The shift in the virulence of the microbial mutualists of ambrosia beetles, from benign nutritional mutualists to phytopathogens, is poorly understood (Hulcr and Dunn 2011). What is clear is that an increase in the number of these ambrosia beetle–related diseases is usually associated with activities that facilitate naive encounters between the beetle-fungus symbiosis and novel plant hosts (Ploetz et al. 2013). More specifically, the emergence of these diseases is largely attributed to the interaction of the beetle's microbial mutualists and novel plant hosts that lack coevolved adaptation (Hulcr and Dunn 2011).

Several of the most prolific ambrosia beetle–related diseases have been examined only once they have become invasive (Cognato et al. 2015; Hughes et al. 2017; Paap et al. 2018). The level of diversity of these invasive species and their microbial mutualists is therefore most likely underrepresented. This is because invasive pests likely undergo "bottleneck" events after introduction and thus represent only a small portion of the diversity present in their natural populations (Stouthamer et al. 2017). This is exemplified by three of the four cryptic species in the *Euwallacea fornicatus* species complex and their primary *Fusarium* fungal mutualists that reside in the Ambrosia *Fusarium* Clade (AFC) (Smith et al. 2019).

Members of the AFC are hypothesized to be the primary symbionts and the main food sources of *Euwallacea* spp. (Kasson et al. 2013; O'Donnell et al. 2015). *Euwallacea* spp.

have also been shown to carry other fungal genera within their mycangia, such as species of *Paracremonium, Graphium*, and *Raffaelea* (Kasson et al. 2013; Lynch et al. 2016; Aoki et al. 2018). To date, 19 AFC species have been identified, several of which were collected in countries outside their native range, particularly in the United States (Freeman et al. 2013; Aoki et al. 2018, 2019; Na et al. 2018). Of these, only eight AFC taxa have been formally described, and only three of these were collected from their native environments (Lynn et al. 2020). Thus, knowledge regarding the fungal mutualists transported within the preoral mycangia of female *E. fornicatus* complex species is largely restricted to invasive populations, which likely represent only a very small segment of the natural diversity (Mendel et al. 2012; Freeman et al. 2013). This has resulted in the previous misleading notion that species in the *E. fornicatus* complex have a strict association with their dominant *Fusarium* spp. associates.

Recent research on members of the *E. fornicatus* complex in their native range of Taiwan showed that the relationship between the species in the *E. fornicatus* complex and the ambrosia fungi they cultivate is likely more diverse and promiscuous than previously described in invaded areas (Carrillo et al. 2019). A recent study by Lynn et al. (2020) on the native ambrosia beetle *E. perbrevis* infesting *A. crassicarpa* trees in Indonesian plantations suggested that a similar pattern of promiscuous symbiosis might occur for that insect. In the present study, 18 different fungal genera were isolated from various ambrosia beetles and their brood galleries, of which several *Fusarium* spp. were most commonly isolated. Because members of the *E. fornicatus* complex have a primary association with *Fusarium* spp. (Kasson et al. 2013; O'Donnell et al. 2015), we hypothesized that *E. perbrevis* is the vector of a more diverse array of *Fusarium* spp. than previously believed. The aim of this study was thus to further investigate the ambrosia beetles previously reported as pests on *A. crassicarpa* in Indonesia and to broaden available knowledge of their fungal mutualists.

MATERIALS AND METHODS

Sample collection and isolation.—

Field surveys of five geographically separated compartments of *A. crassicarpa* plantations in Riau, Indonesia, showing ambrosia beetle infestation were conducted during 2018 and 2019. Three moderately (10–30 entry holes) and three highly (>31 entry holes) infested, 2- to 3-y-old living trees were selected at each site, felled 50 cm above ground level, and cut into 50 cm billets. These billets were immediately transported to the laboratory, where they were split with sterilized equipment, and living female beetles were extracted and placed in conical screw cap tubes containing sterile filter paper. Each tube contained five beetles that were grouped based on morphology and stored for later identification and mycangial fungus isolation. Compartments surveyed are summarized in SUPPLEMENTARY TABLE 1.

Fungal isolates used in this study were either obtained from the heads of female beetles (where the preoral mycangium is located) using methods similar to those described by Lynch et al. (2016) or by culturing them from the surfaces of the beetle galleries using methods described by Eskalen et al. (2013). For the mycangial extractions, beetles were surface-disinfected by submerging individual specimens in Eppendorf tubes containing 70% (*v*/*v*) ethanol. Tubes were agitated with a vortex mixer for 20 s, rinsed with sterile deionized water, and allowed to air-dry on sterile filter paper under a laminar-flow chamber.

Beetle heads were separated from the thoracic and abdominal segments under a dissection microscope and then individually macerated in sterile 1.5-mL microcentrifuge tubes with sterile surgical tweezers. To select for *Fusarium* spp., the macerated heads were processed in one of two ways: (i) the macerated heads were smeared directly onto the surface of *Fusarium* selective medium agar (FSM; Leslie and Summerell 2006) amended with 100 μg L^{-1} streptomycin sulfate (Sigma, Steinheim, Germany) or (ii) they were suspended in 200 μL of sterile water in 1.5-mL Eppendorf tubes, shaken for 10 s, and 50 μL of the supernatant pipetted and spread onto FSM plates amended with 100 μg L^{-1} streptomycin sulfate (Sigma), using sterile glass rods. The Petri dishes were incubated at 25 C for 3–5 d to allow for fungal growth.

Fungal colonies having unique morphologies were subcultured onto 2% malt extract agar (MEA; 20 g/L malt extract, 20 g/L agar, Biolab, Midrand, South Africa), amended with 100 μg L^{-1} streptomycin. To obtain pure colonies for further downstream identification, single-hyphal-tip cultures were made onto MEA 5 d post subculturing. The remaining thoracic and abdominal segments of the dissected beetles were individually stored in 200 μL of 70% (*v*/*v*) ethanol for downstream beetle identification. Care was taken to store the beetles accurately so as to link the fungi to the beetles from which they had been isolated.

All cultures obtained in this study were deposited in the culture collection (CMW) of the Forestry and Agricultural Biotechnology Institute (FABI), University of Pretoria, Pretoria, South Africa. A subset of these were selected from further downstream analysis (SUPPLEMENTARY TABLE 2). Representative isolates of novel taxa were deposited in the culture collection (CBS) of the Westerdijk Fungal Biodiversity Institute, Utrecht, The Netherlands.

DNA extraction, PCR, and phylogenetic analyses.—

Beetle specimens. DNA was extracted from both wings and two legs of stored beetle specimens using the prepGEM Universal DNA extraction kit (ZyGEM, Biocom Africa, Centurion, South Africa), following the manufacturer's protocol, with the exception that the final product was not diluted. The extracted DNA was used for polymerase chain reaction (PCR) amplification of the mitochondrial cytochrome oxidase *c* subunit I gene (*COI*), using the primer pair LCOI490 and HCO2198 (Folmer et al. 1994). Each PCR reaction mixture consisted of 2.5 μL 5× MyTaq buffer (Bioline, London, UK), 0.25 μL MyTaq DNA polymerases (Bioline), 1 μL DNA template, 0.5 μL of each primer (10 mM), and 8.25 μL of sterile deionized water, for a 13-μL total reaction mixture. PCR amplification protocols were the same as those described by Lynn et al. (2020), for all the beetle specimens. Successful amplification was confirmed by staining 2 μL PCR product with 2 μL GelRed Nucleic Acid Gel Stain (Biotium, Hayward, California) and separating them by electrophoresis on a 2% agarose gel, followed by visualization under ultraviolet (UV) light.

PCR products were purified using 6% Sephadex G-50 columns following the manufacturer's protocols (Sigma-Aldrich, Steinheim, Germany). Products were sequenced in both directions in 10-μL reactions, using the same primers used for PCR amplification. The reaction mixture contained 1 μL BigDye Terminator 3.1 Ready Reaction Mix (PerkinElmer, Warrington, UK), 1 μL sequencing buffer, 0.5 μL of either the forward or the reverse primer (10 mM) for the *COI* gene region, 1 μL cleaned PCR product, and 6.5 μL of sterile deionized water. The thermal cycling conditions included 25 cycles of 10 s at 96 C, 5 s at 55 C, and 4 min at 60 C. Sequencing products were cleaned using Sephadex G-50 columns and dried in an Eppendorf

5301 vacuum concentrator at 60 C for 5 min. Sequencing was performed at the sequencing facility of the University of Pretoria, on an ABI Prism 3500xl autosequencer (Applied Biosystems, Foster City, California). The forward and reverse sequencing reads were assembled into contigs using CLC Bio Main Workbench 6 (CLC Bio, www.clcbio.com), and the consensus sequences were extracted and exported for phylogenetic analyses.

A preliminary identity for the beetle specimens was obtained by performing a nucleotide BLAST of the *COI* sequences against the National Center for Biotechnology Information (NCBI) GenBank database (http://www.ncbi.nlm.nih.gov). Based on the results, sequences of closely related taxa were downloaded and incorporated into data sets provided by Lynn et al. (2020) and used for phylogenetic analyses. Sequence alignments for the gene region were generated using MAFFT 7 (Katoh and Standley 2013) and manually checked and corrected where necessary using MEGA 7 (Kumar et al. 2016). Genealogical relationships among individual beetles were reconstructed using maximum likelihood (ML) analyses, which were executed on the online CIPRES Science Gateway 3.3 platform (Miller et al. 2010), using the online RAxML-HPC BlackBox 8.2.10 tool (Stamatakis 2014), with default parameters. A nonparametric analysis of the sequence data with 1000 bootstrap replicates provided statistical support for the branches of the generated ML trees. *Ambrosiophilus sexdentatus* (HM06405) was used to root the ML analysis as suggested by Gomez et al. (2018).

The DNA sequences for the representative specimens sequenced in this study are stored in the Entomological DNA collection at the Forestry and Agricultural Biotechnology Institute (FABI), University of Pretoria, South Africa (SUPPLEMENTARY TABLE 1). All additional specimens collected in this study are stored in 70% (*v*/*v*) ethanol in the Scolytine beetle collection at FABI, University of Pretoria, South Africa.

Fungal isolates. Genomic DNA of 3-d-old cultures was extracted from all isolates resembling *Fusarium* spp. obtained from the preoral mycangia located in the heads of female *Euwallacea* beetles and their corresponding brood galleries (Spahr et al. 2020). For this purpose, 50 µL of the Prepman Ultra Sample Preparation Reagent (Thermo Fisher Scientific, Waltham, Massachusetts) was used, following the manufacturer's protocols. The resulting extracted suspension was diluted with 200 µL of sterile deionized water. PCR amplification was performed for four gene regions as follows: (i) the ribosomal internal transcribed spacer region and the domains D1 and D2, at the 5′ end of the nuclear large subunit (ITS1-5.8S-ITS2 + 28S rDNA), using the primer pairs ITS4/ITS5 (White et al. 1990) and NL1/NL4 (Kurtzman and Robnett 1997), respectively; (ii) the translation elongation factor 1-α (*TEF1-α*), using the primer pair EF1/EF2 (O'Donnell et al. 1998); (iii) the RNA polymerase subunit I (*RPB1*), using the primer pairs F5/R8 (*RPB1-1*) (O'Donnell et al. 2010) and F7/G2R (*RPB1-2*) (O'Donnell et al. 2010); and (iv) the RNA polymerase subunit II (*RPB2*), using the primer pairs 5F2/7CR (*RPB2-1*) and 7CF/11AR (*RPB2-2*) (O'Donnell et al. 2007). PCR amplifications were performed in 13-µL reactions containing 2.5 µL 5× MyTaq buffer (Bioline), 0.25 µL MyTaq DNA polymerases (Bioline), 1 µL DNA template, 0.5 µL of each primer (10 mM), and 8.25 µL of sterile deionized water. PCR was performed for each primer pair using published cycling parameters (White et al. 1990; O'Donnell and Cigelnik 1997; Jacobs et al. 2004; O'Donnell et al. 2007). Amplification of products was confirmed with gel electrophoresis as described above.

PCR products were purified using 6% Sephadex G-50 columns following the manufacturer's protocols (Sigma-Aldrich) and sequenced and assembled using the same protocols described above. The extracted consensus sequences were exported for phylogenetic analyses. Initial

BLAST searches against the NCBI GenBank database of the resulting translation elongation factor 1-α (*TEF1-α*) sequences were performed to confirm that the isolates were those of *Fusarium* spp. The confirmed sequences were then combined with the data sets generated by Lynn et al. (2020) (SUPPLEMENTARY TABLE 2), to construct data sets for phylogenetic analyses. DNA sequences for the ITS-28S rDNA, *TEF1-α*, and *RPB2* gene regions obtained in this study were individually compiled with each respective gene data set, aligned, and inspected following the same procedures described above for the beetles. The individual data sets were combined using FASconCAT-G (Kück and Longo 2014).

Phylogenetic analyses of *Fusarium* spp. were conducted using concatenated DNA sequences of the ITS-28S rDNA, *TEF1-α*, and *RPB2* gene regions from 40 isolates of *Fusarium* spp. obtained in this study. In addition, sequences were obtained from GenBank for 88 isolates previously used in AFC phylogenetic analyses (Kasson et al. 2013; Carrillo et al. 2019; Sandoval-Denis et al. 2019; Lynn et al. 2020) (SUPPLEMENTARY TABLE 2). Maximum likelihood (ML) analyses were performed using the online CIPRES Science Gateway 3.3 platform (Miller et al. 2010) and with the online RAxML-HPC BlackBox 8.2.10 tool (Stamatakis 2014). Maximum likelihood analyses were carried out using the GTRGAMMA+I substitution model, with all other parameters set to default. Statistical support for the branches in the ML trees was obtained by performing 1000 bootstrap replicates. *Fusarium neocosmosporiellum* (NRRL 22468) and *Fusarium lichenicola* (NRRL 32434) were used as the outgroups based on previous studies (Kasson et al. 2013; O'Donnell et al. 2015).

Morphological characterization of *Fusarium* spp.—

For morphological characterization, isolates of *Fusarium* spp. were grown on potato dextrose agar (PDA; PDA 20 g/L; BD Difco, Berkshire, UK) and synthetic low-nutrient agar (SNA; including 0.2 g glucose, 0.2 g sucrose, 1 g KH_2PO_4, 1 g KNO_3, 0.5 g $MgSO_4 \cdot 7H_2O$, 0.5 g KCl, 20 g Difco agar per liter; Leslie and Summerell 2006). Cultures were incubated in either darkness, or under continuous UV light, or under an ambient day/light photoperiod. Under all three different light conditions, cultures were grown at ambient room temperature (23–25 C) for 14 d and used to evaluate the characteristic traits for this group of fungi (Aoki et al. 2005; Freeman et al. 2013). Microscope slides were prepared for each isolate, with structures mounted in distilled water, and 25–50 measurements were recorded for each defining characteristic using a Nikon H550L microscope (Nikon, Yokohama, Japan). Conidia and conidiophores produced on SNA under continuous black light were either mounted in water or observed directly on the agar plates to which a coverslip had been added and then examined and photographed. Photographs and photo plates were edited and assembled in Adobe Photoshop CS (San Jose, USA), respectively. Images of conidia in focus were also orientated into a linear arrangement in Adobe Photoshop CS. Extreme care was taken to ensure that defining characteristics were not morphologically manipulated in any way. Means, standard deviations, standard errors, maximum and minimum values for the microscopic characters were calculated and presented as minimum–(mean minus standard deviation)–mean–(mean plus standard deviation)–maximum.

To determine optimum growth conditions for growth in culture, colony growth rates for each representative isolate were determined. Three replicates of each of these isolates were assessed at six temperatures ranging from 10 to 35 C at 5 C intervals grown in the dark. Agar plugs (5 mm diam) were cut from the edges of 1-wk-old cultures and placed at the centers of 90-mm Petri dishes containing PDA. Two measurements of colony diameter perpendicular to

each other were made every day for 10 d, after which averages were determined. Cultures incubated for 14 d and for 1 mo at 25 C in the dark and in ambient daylight on PDA in 90-mm Petri dishes were used to characterize colony color (surface and reverse), odor, and morphology. Colony colors (surface and reverse) were described using the color charts of Rayner (1970).

Figure 1. *Euwallacea perbrevis* and *Euwallacea similis*. A. Mature female *Euwallacea perbrevis* (TSHBa) beetle collected from infested *Acacia crassicarpa* in Indonesia. B. Mature female *Euwallacea similis* beetle collected from infested *Acacia crassicarpa* in Indonesia. Bars = 1.0 mm. Images provided by Dr. Andrew J. Johnson and Dr. You Li from the Forest Entomology Laboratory, University of Florida, Gainesville

RESULTS

Beetle specimen collection and fungal isolations.—

A total of 114 living adult *Euwallacea* spp. female beetles were extracted from 30 infested logs collected from the five sampled compartments. Morphological identification using the online Southeast Asia ambrosia beetle identification resource (http://idtools.org/id/wbb/sea-ambrosia/index.php) identified *Euwallacea perbrevis* (TSHBa; FIG. 1A) and *E. similis* (FIG. 1B) as the most abundant beetle species present. Isolations from the mycangia of these beetles and their corresponding brood galleries yielded 157 (114 isolated from the beetle mycangia and 43 from the brood galleries) fungal isolates that had morphological characteristics typical of *Fusarium* spp.

PCR amplification and sequencing.—

Beetle specimens. Maximum likelihood phylogenetic analysis of the beetle *COI* sequence data (146 taxa, 569 characters) (FIG. 2) confirmed that *Euwallacea perbrevis* (TSHBa) and *E. similis* were the most abundant beetle species present in the sampled trees. Three distinct *COI* haplotypes (FIG. 2) of *E. perbrevis* were obtained, one of which had not previously been described. All three of these haplotypes grouped into the same clade as other specimens collected from Indonesia (Gomez et al. 2018; Lynn et al. 2020), with 100% bootstrap support. The *E. perbrevis* specimens sequenced and identified as haplotype A in this study were the most commonly collected *E. perbrevis* haplotype and had the widest distribution, as they were collected from four of the five sampled compartments (SUPPLEMENTARY TABLE 1). In contrast, haplotype C and the novel haplotype B were less abundant and were collected only in two of the five sampled compartments.

Among the *E. similis* specimens sequenced in this study, four novel *COI* haplotypes were identified (FIG. 2). Novel haplotypes D and F were the least abundant haplotypes, each with only one representative specimen collected from a single, but different compartment each. Novel haplotype E was collected from three compartments and was the most widely distributed. Haplotype G was the most commonly collected and was found in two different compartments. The aligned data set for *COI* (146 taxa, 569 characters) was deposited in TreeBASE (http://purl.org/phylo/treebase/phylows/study/TB2:S26378). All sequences obtained for the beetle specimens sequenced in this study were deposited in GenBank (SUPPLEMENTARY TABLE 1).

Fungal isolates. PCR amplification of the RNA polymerase subunit I (*RPB1*), using the primer pairs F5/R8 (*RPB1-1*) and F7/G2R (*RPB1-2*) (O'Donnell et al. 2010), was not uniformly successful for all isolates. The amplicon lengths for the ITS-28S rDNA, *TEF1-α*, and *RPB2* gene regions that successfully amplified were approximately 1100, 700, and 1400 bp, respectively. The combined multilocus data set included 128 taxa and 1824 characters (*TEF1-α* = 278, ITS-28S = 401, *RPB2* = 1145), including alignment gaps. Of the 1824 characters, 204 were phylogenetically informative. Isolates sequenced in this study and incorporated into the final data sets were deposited in GenBank (SUPPLEMENTARY TABLE 2). The aligned sequences for the ITS-28S rDNA, *RPB2, TEF1-α*, and combined ITS-28, *RPB2*, and *TEF1-α* data sets were deposited in TreeBASE (http://purl.org/phylo/treebase/phylows/study/TB2:S26376). Separate trees for each partition are presented as SUPPLEMENTARY FIGS. 1–3.

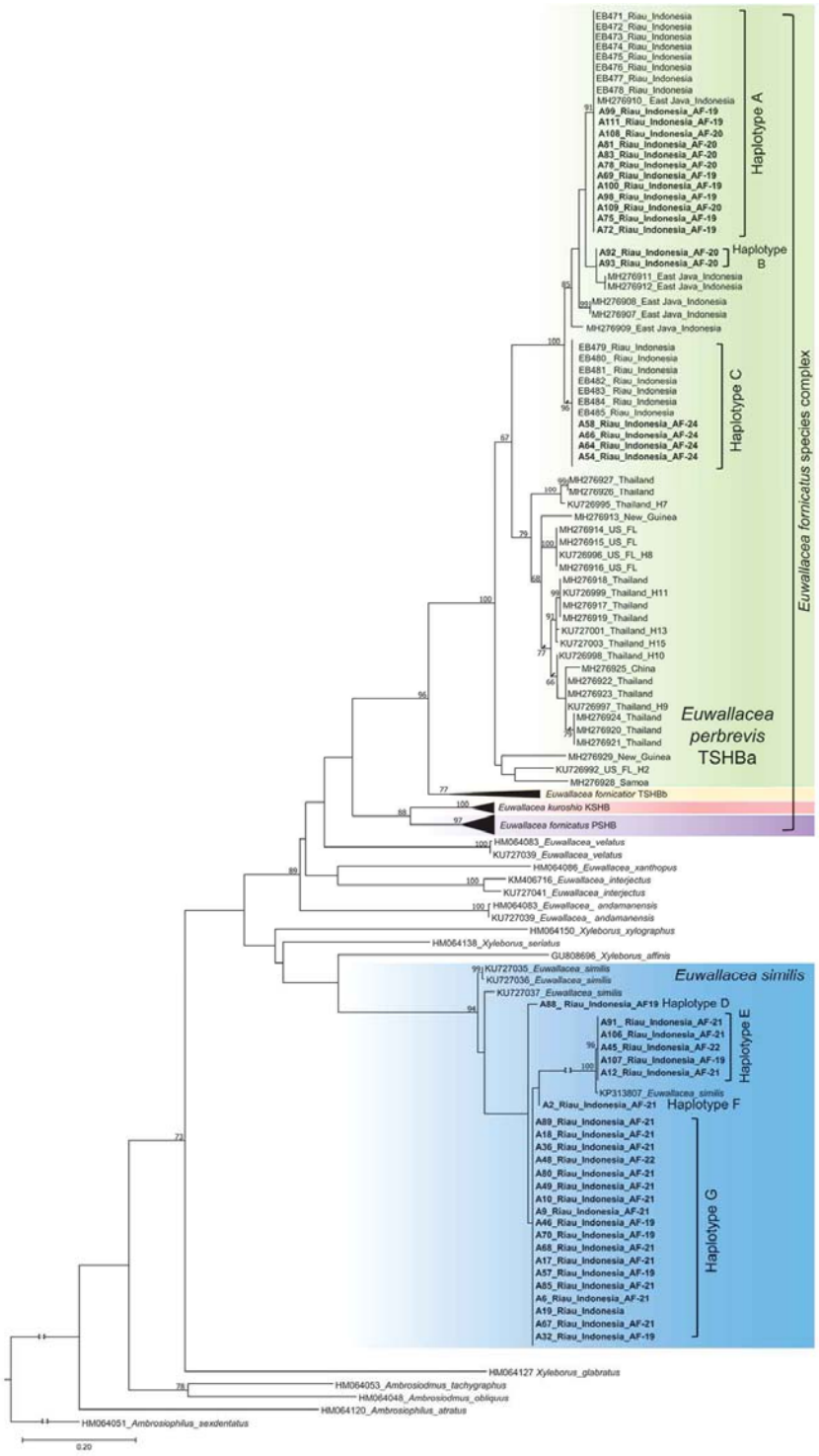

Figure 2. Phylogenetic tree based on maximum likelihood (ML) analysis of *COI* gene sequences for various ambrosia beetle species in the *Euwallacea fornicatus* species complex (Gomez et al. 2018). Specimens in bold were sequenced in this study. Support for bootstrap values above 60% are presented at the nodes. Three distinct haplotypes of *E. perbrevis* where identified, one of which was novel (haplotype B), but all grouped with the other specimens collected from Indonesia with 100% bootstrap support. Four distinct novel haplotypes of *E. similis* were identified, indicating a high amount of genetic variation within this species. The AFC members associated with the beetles sequenced in this study are indicated where known. *Ambrosiophilus sexdentatus* (HM064051) represents the outgroup

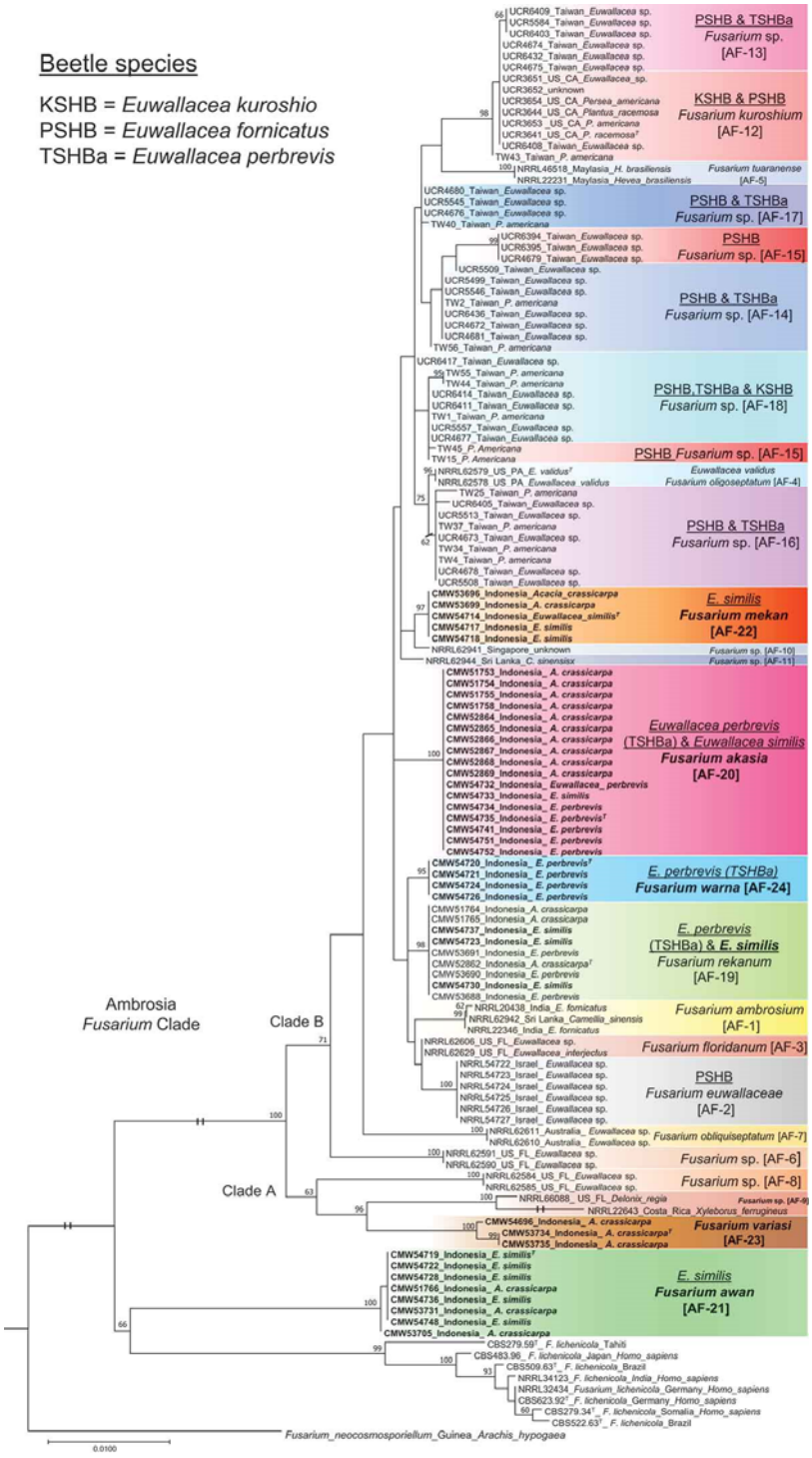

Figure 3. Multilocus phylogenetic analysis of the species in the Ambrosia Fusarium Clade (AFC) using combined sequences from the ITS-28S rDNA, *TEF1-α*, and *RPB2* gene regions. The phylogram was constructed using maximum likelihood with 1000 bootstrap replicates. Support for bootstrap values above 60% are presented at the nodes. Isolates in bold were sequenced in this study. Two early diverging monophyletic sister clades are identified as clades A and B. The highlighted boxes indicate the 23 species within the AFC, including the new species described in this study, and the 23 species are identified as AF-1 through to AF-23 using an ad hoc nomenclature (Na et al. 2018; Carrillo et al. 2019). The beetle vector(s) of the AFC fusaria is indicated where known. *Fusarium neocosmosporiellum* (NRRL 22468) represents the outgroup. T represents ex-holotype cultures

Multilocus phylogenetic analyses based on three loci (ITS-28S rDNA, *TEF1-α*, and *RPB2*) (FIG. 3) showed that the *Fusarium* spp. recovered from *Euwallacea* spp. represented five AFC species, including *F. rekanum* and four novel AFC species (AF-20 to AF-23). One novel *Fusarium* spp. grouping just outside of the AFC, but still within the greater *Fusarium solani* species complex (FSSC), was also identified. Three of these novel AFC members reside in AFC species clade B (AF-20, AF-21, and AF-23), one in clade A (AF-22), and the remaining novel species fell outside clades A and B, forming a sister clade with *F. lichenicola* (NRRL 32434) (Kasson et al. 2013; O'Donnell et al. 2015).

RPB2 was the most informative gene region in the phylogenetic analyses, providing high bootstrap support for 13 of the 23 AFC species, including four of the five novel lineages (AF-20, AF-22, AF-23, and the novel non-AFC mutualist) (SUPPLEMENTARY FIG. 1). In contrast, bootstrap analysis of the ITS-28 provided the weakest signal and resolved only 5 of the 23 AFC species, including the novel non-AFC mutualist and AF-22 (SUPPLEMENTARY FIG. 2). The combined analyses of ITS-28, *RPB2*, and *TEF1-α* provided the strongest support for the evolutionary relationships within members of the AFC, with high bootstrap support for 16 of the 23 AFC species.

The topology of the ML phylogram based on the combined data set differed from that in a previous study by Carrillo et al. (2019). Unlike their analyses, we excluded the *RPB1* gene region because we were unable to successfully amplify this gene region for almost all isolates and rather included the 28S rDNA gene region. Major groupings within both analyses were, however, similar. Bootstrap support for the two AFC clades (clades A and B of Kasson et al. 2013) was robust. However, ML bootstrapping failed to support most of the nodes along the backbone of the phylogeny. Fifteen of the species lineages represented by two or more isolates were strongly supported as genealogically exclusive (FIG. 3). The only exceptions were for AF-3, AF-12, AF-13, AF-15 and AF-18 (FIG. 3).

Representative isolates of the novel species were deposited in the living collection (PPRI) of the South African National Collection of Fungi (NCF), Roodeplaat, South Africa. Dried specimens of sporulating cultures were deposited in the herbarium collection (PREM) of the South African National Collection of Fungi, Roodeplaat, South Africa.

TAXONOMY

Based on multilocus phylogenetic analyses and a detailed comparison of phenotypic/morphological characters, four novel AFC species and one novel *Fusarium* sp. mutualist, all in the *Fusarium solani* species complex (FSSC), are described.

Fusarium akasia Lynn & I. Barnes, sp. nov. FIG. 4

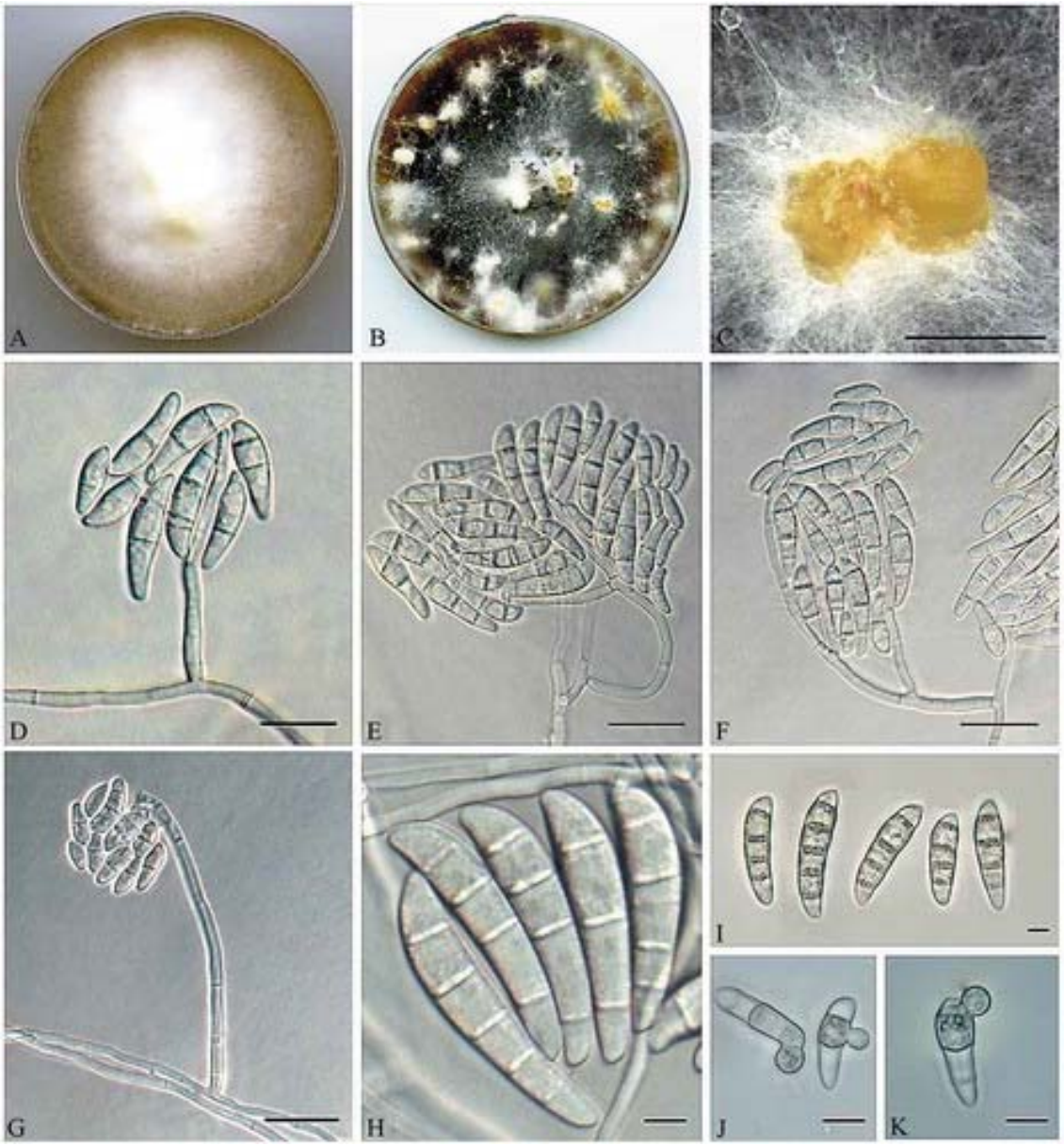

Figure 4. Morphological characteristics of *Fusarium akasia* on PDA and SNA (CMW 54735, CMW 54741, and CMW 54752). A–C, I–K. Morphology of *F. akasia* cultures grown on potato dextrose agar (PDA). D–H. Morphology of 14-d-old *F. akasia* cultures grown on synthetic low-nutrient agar (SNA). A. Colony morphology on PDA at 2 wk. B–C. Luteous-ochreous conidial masses formed in culture on PDA after 1 mo. D–G. Simple to branched aerial conidiophores forming multiseptated conidia, often swollen apically with 1–5 septa or oval to short-clavate with 0–2 septa. H. Curved clavate multiseptated aerial conidia with 3–5 septa that are morphologically indistinguishable from sporodochial conidia. I. Multiseptate sporodochial conidia with bulging appearance and a round, blunt apical cell, and a barely notched, distinct, foot-like basal cell, with 4–5 septa. J–K. Multiseptate conidia with round to oval, rough-walled, ridged appearance, chlamydospore formation. Bars: C = 1 mm; D–G = 30 µm; H–I = 5 µm; J–K = 10 µm

MycoBank MB834436

Typification: INDONESIA. RIAU: Pelalawan, *Acacia crassicarpa* plantation, isolated from the head (including mycangium) of a *Euwallacea perbrevis* (TSHBa) specimen, Mar 2019, *K.M.T. Lynn* (**holotype** PREM 62607). Ex-type strain CMW 54735 = PPRI 27978 = CBS

146880. GenBank: ITS-28S rDNA = MN954357; *TEF1-α* = MT009971; *RPB*2-1 = MT009931; *RPB*2-2 = MT010011.

Etymology: The name *akasia* is derived from the Bahasa Indonesia word "akasia" meaning *Acacia*. It reflects the plant host infested and damaged by the beetle vectors, *E. perbrevis* and *E. similis*.

Culture characteristics: Colony color on PDA white, buff (pale yellow) to saffron (light orange yellow) or fulvous in dark, buff to honey darkening to red, blood red after 1 mo in ambient daylight. Colony margin on PDA at 14 d entire, occasionally lobate or curled/concentric, colony elevation convex to umbonate. Reverse pigmentation yellowish white to buff darkening to isabelline or cinnamon in dark, saffron to orange darkening to rust and blood red after 1 mo in ambient daylight. Odor absent. Occasional apricot to red exudates. Colonies on PDA radial mycelial growth rates of an average of 2.59 mm/d at 15 C, 4.83 mm/d at 20 C, 7.34 mm/d at 25 C, 7.48 mm/d at 30 C, and 1.28 mm/d at 35 C in dark. Conidial pustules, produced on sporodochia, form on older cultures grown on PDA and are luteous to ochreous. Aerial mycelium sparse with pionnotal colony appearance, or abundant, loose to floccose, white to buff. Chlamydospores formed sparsely in hyphae, often in mature conidia, mostly round to oval, intercalary, often single or paired, ordinary hyaline, smooth, often rough-walled, 2–(5)–8–(11)–13 × 2–(6)–8–(10)–10.5 µm. Sclerotia absent. Sporulation on SNA abundant, particularly under UV light, slow on PDA. Sporodochia formed sparsely on SNA, abundantly on PDA. Aerial conidiophores formed abundantly on SNA and PDA, often arched, varying in length, thick with slight tapering toward the apex and the base, often branched, 31–(36)–87–(138)–219 × 3–(5)–6–(7)–8 µm, forming monophialides integrated in apices. Aerial phialides simple, subcylindrical, with discreet collarette. Aerial conidia (i) mostly oval, 2-celled oval to obovoid, slightly curved, short-clavate with truncated bases, 0–1(–2) septa, 10.5–(13)–16–(19)–22 × 4–(5)–6–(7)–10 µm; (ii) clavate, sometimes slightly curved cylindrical, (0–)1–4(–5)-septate conidia, morphologically similar to the clavate sporodochial conidia. Sporodochial conidiophores thick with slight bulging at midsection, often branched, forming apical monophialides. Sporodochial phialides simple, subcylindrical with crooked tube shape and discreet collarette. Sporodochial conidia ordinarily hyaline, mostly slightly curved clavate, ridged appearance, swollen in upper parts, tapering toward the base, often with a round, blunt apical cell, and a barely notched, foot-like basal cell, (0–)1–4(5)-septate, formed on PDA and SNA, 22–(28)–35–(42)–49 × 6–(8)–10–(12)–13 µm. Short-clavate to obovate, straight or curved conidia, with rounded apex and truncate base, 0–1-septate, sometimes formed together with multiseptate conidia borne on thick sporodochial conidiophores.

Habitat: Acacia crassicarpa plantations infested with ambrosia beetles in Riau, Indonesia.

Known distribution: Riau, Indonesia.

Additional specimens examined: INDONESIA. RIAU: Pelalawan, *Acacia crassicarpa* plantation, isolated from the head (including mycangium) of a *Euwallacea perbrevis* (TSHBa) specimen, Mar 2019, *K.M.T. Lynn*, **paratype** PREM 62608, ex-type culture CMW 54741 = PPRI 27979 = CBS 146881; ibid., Mar 2019, *K.M.T. Lynn*, **paratype** PREM 62609, ex-type culture CMW 54752 = PPRI 27980 = CBS 147161.

Diagnosis: The species is easily distinguished by its clavate sporodochial conidia that have a ridged bulging appearance. The abundance of the arched thick aerial conidiophores that taper

slightly at the base is also a diagnostic feature. This species resides in clade B of the AFC. It is phylogenetically distinct from other previously described AFC species based on a maximum likelihood analysis using the *RPB2* gene region (SUPPLEMENTARY FIG. 1) and a multilocus analysis using three loci (ITS-28S rDNA, *TEF1-α*, and *RPB2*) (FIG. 3).

Fusarium awan Lynn & I. Barnes, sp. nov. FIG. 5

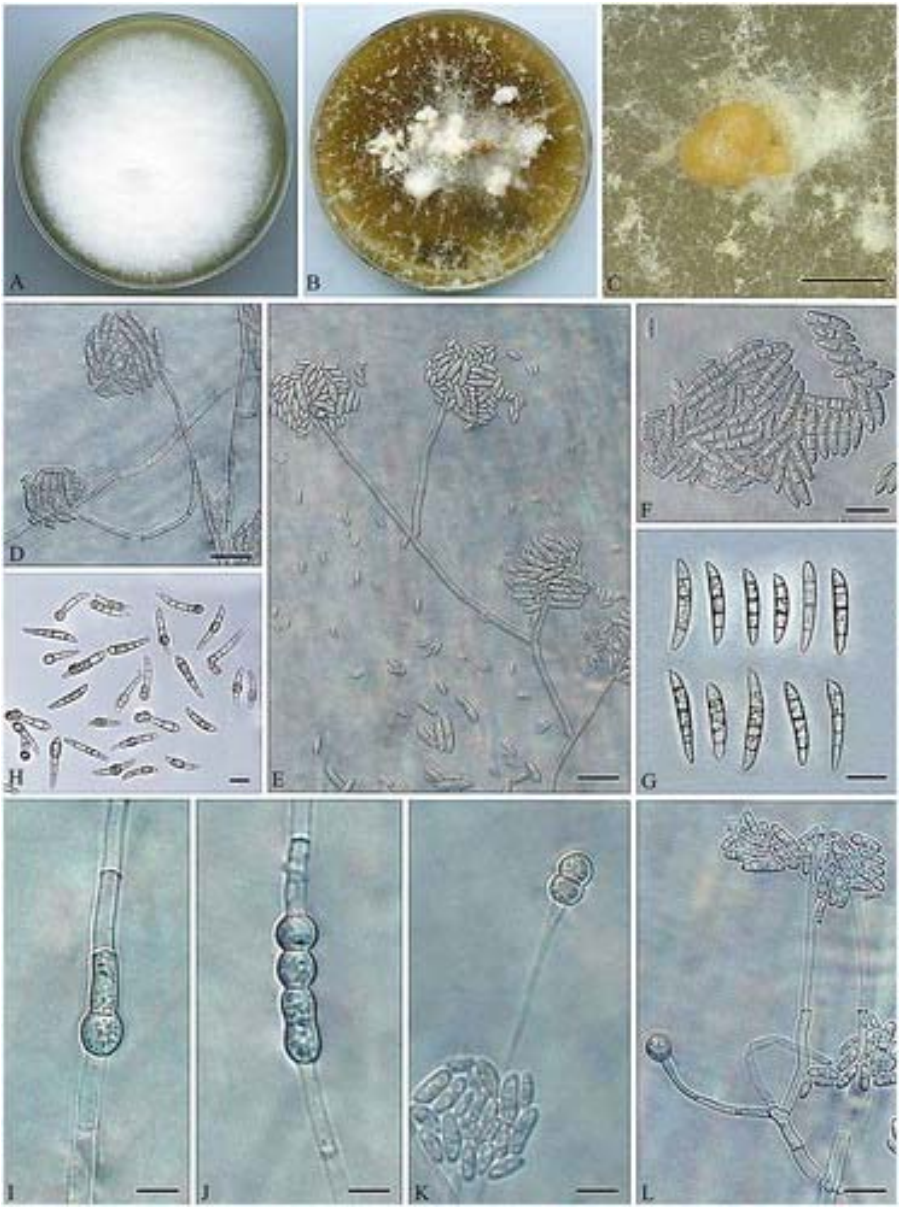

Figure 5. Morphological characteristics of *Fusarium awan* on PDA and SNA (CMW 54719, CMW 53705, and CMW 54722). A–C, G–H. Morphology of *F. awan* cultures grown on potato dextrose agar (PDA). D–F, I–L. Morphology of 14-d-old *F. awan* cultures grown on synthetic low-nutrient agar (SNA). A. Colony morphology on PDA at 2 wk. B–C. Luteous-ochreous conidial masses formed in culture on PDA after 1 mo. D–E. Mature multiseptated conidia with 0–3 septa, formed on branched aerial conidiophores. F. Long, barely curved, flute-shaped multiseptated aerial conidia with 0–3 septa that are morphologically similar to sporodochial conidia. G. Multiseptate narrow sporodochial conidia with a round or papillate apical cell, and a barely notched, foot-like basal cell, with 3–4 septa. H–L. Round to oval chlamydospores, single, paired or in chains, formed intercalary or terminally in hyphae or in mature narrow conidia. Bars: C = 2 mm. D-E = 20 µm; F-G = 15 µm; H-L = 10 µm

MycoBank MB834437

Typification: INDONESIA. RIAU: Pelalawan, *Acacia crassicarpa* plantation, isolated from the head (including mycangium) of a *Euwallacea similis* specimen, Mar 2019, *K.M.T. Lynn* (**holotype** PREM 62602). Ex-type strain CMW 54719 = PPRI 27973 = CBS 146882. GenBank: ITS-28S rDNA = MN954345; *TEF1-α* = MT009959; *RPB*2-1 = MT009919; *RPB*2-2 = MT009999.

Etymology: The name *awan* is derived from the Bahasa Indonesia word "awan" meaning cloud and reflects the white mycelial growth of the fungus on the yellowish agar. Thus, the fungi in culture appear as sun shining through large white cumulus clouds.

Culture characteristics: Colony color on PDA white in dark, white darkening to honey after 1 mo in ambient daylight. Colony margin on PDA after 14 d entire, occasionally curled, particularly under ambient daylight, colony flat, often irregularly umbonate. Reverse pigmentation yellowish white to buff in dark, buff darkening to ochreous after 1 mo in ambient daylight. Odor absent. Exudates absent. Colonies on PDA radial mycelial growth rates of average 1.44 mm/d at 15 C, 4.54 mm/d at 20 C, 6.12 mm/d at 25 C, 6.57 mm/d at 30 C, and 3.26 mm/d at 35 C in dark. Conidial pustules luteous to ochreous, produced on sporodochia that form in older cultures on PDA. Aerial mycelium sparse with pionnotal colony appearance, or abundant, loose to floccose, white to buff. Chlamydospores abundant in hyphae and in mature conidia, mostly oval to round ellipsoidal, intercalary or terminal, often single or paired, occasionally in chains, ordinary hyaline, smooth, often rough-walled, 4–(6)–7–(8)–10 × 5–(6)–7–(8)–10 µm. Sclerotia absent. Sporulation on SNA abundant, particularly under UV light, retarded on PDA. Sporodochia sparse on SNA, abundant on PDA. Aerial conidiophores abundant on SNA and PDA, often with multiple branching, varying in length, with slight tapering toward the apex, 47–(69)–120–(171)–245 × 2–(3)–4–(5)–6 µm, forming monophialides integrated in apices. Aerial phialides simple, subcylindrical, with discreet collarette. Aerial conidia of two forms: (i) mostly oval, 2-celled and 3-celled oval, 0–1(2) septa, 8–(11)–13–(15)–20 × 3–(3)–4–(5)–6 µm; (ii) long, barely curved, flute-shaped with discreet tapering toward the base, 1–3-septate conidia, 12–(20)–24–(28)–31 × 3–(4)–5–(6)–8 µm. Sporodochial conidiophores thick, often branched, forming apical monophialides. Sporodochial phialides simple, subcylindrical, tube-shaped, with discreet collarette. Sporodochial conidia hyaline, varying in shape and size: (i) curved, narrow, cylindrical or slightly clavate, often swollen in upper parts with narrow papillate apical cells, tapering abruptly toward the base, with barely notched, foot-like basal cell, or simply rounded at base, often abundantly producing chlamydospores, 2–4 septa, 19.5–(27)–35–(43)–36 × 3.5–(4.5)–5.5–(6.5)–8 µm; (ii) ordinarily hyaline, barely curved, flute-shaped, no or slight tapering toward the base, often with round, blunt apical cell, and barely notched, foot-like basal cell, 0–2–3(–4)-septate, 14–(21)–25–(29)–33 × 3–(3.5)–4.5–(5.5)–7 µm. Short-clavate to oval, straight or slightly curved conidia, with rounded apex, occasionally truncate base, 0–1-septate, often formed together with multiseptate conidia borne on thick sporodochial conidiophores.

Habitat: A. crassicarpa plantations infested with ambrosia beetles in Riau, Indonesia.

Known distribution: Riau, Indonesia.

Additional specimens examined: INDONESIA. RIAU: Pelalawan, *Acacia crassicarpa* plantation, isolated from *A. crassicarpa* infested with *E. perbrevis* (TSHBa) and *E. similis*,

Nov 2018, *K.M.T. Lynn*, **paratype** PREM 62594, ex-type culture CMW 53705 = PPRI 27957 = CBS 146883; ibid., isolated from the head (including mycangium) of a *Euwallacea similis* specimen, Mar 2019, *K.M.T. Lynn*, **paratype** PREM 62604, ex-type culture CMW 54722 = PPRI 27975 = CBS 146884.

Diagnosis: The species has abundant chlamydospores both in the hyphae and within mature conidia. It can also be recognized by the formation of multiseptate aerial conidia having an elongated oval shape and by the production of very narrow sporodochial conidia compared with other *Euwallacea-Fusarium* mutualists. This species is also, to the best of our knowledge, the first *Fusarium* mutualist isolated from the mycangia of a *Euwallacea* beetle that does not group phylogenetically within the AFC, but still within the FSSC. This species is phylogenetically distinct from other previously described FSSC species based on individual maximum likelihood analyses using the *RPB2* and *TEF1-α* gene regions, respectively, as well as a multilocus analysis using three loci (ITS-28S rDNA, *TEF1-α*, and *RPB2*). Within the AFC, this species can be phylogenetically distinguished from other previously described species based on individual (SUPPLEMENTARY FIGS. 1–3) and combined analyses of the ITS-28S rDNA, *TEF1-α*, and *RPB2* gene regions (FIG. 3), respectively.

Fusarium mekan Lynn & I. Barnes, sp. nov.FIG. 6

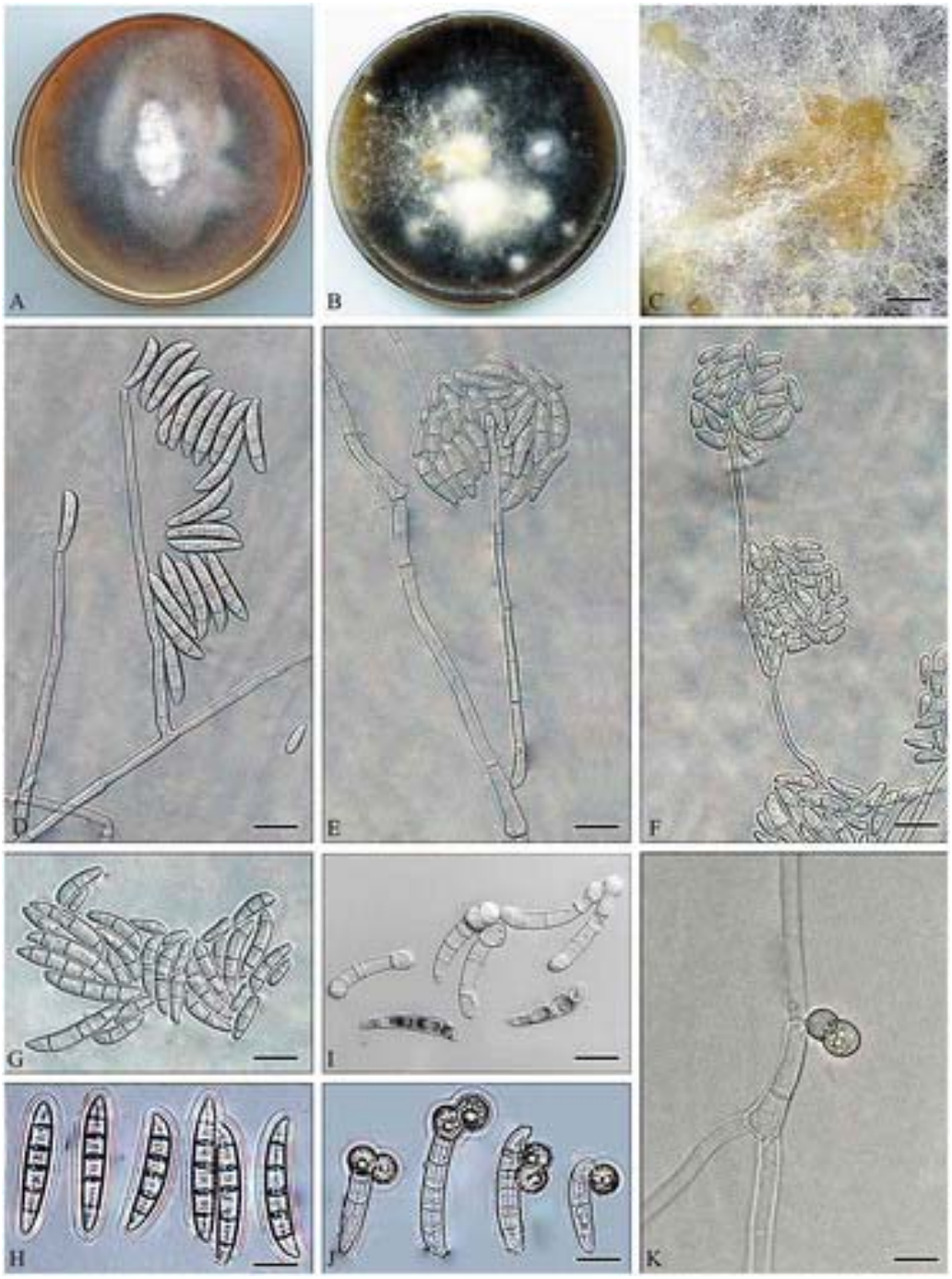

Figure 6. Morphological characteristics of *Fusarium mekan* on PDA and SNA (CMW 54714, CMW 53696, and CMW 54717). A–C, H–J. Morphology of *F. mekan* cultures grown on potato dextrose agar (PDA). D–G, K. Morphology of 14-d-old *F. mekan* cultures grown on synthetic low-nutrient agar (SNA). A. Colony morphology on PDA at 2 wk. B–C. Luteous-ochreous conidial masses formed in culture on PDA after 1 mo. D–F. Simple to branched aerial conidiophores forming multiseptated conidia, often slightly swollen apically with 1–5 septa or oval to short-clavate with 0–1 septa. G. Slightly curved multiseptated aerial conidia with 2–4 septa that are morphologically indistinguishable from sporodochial conidia. H. Multiseptate sporodochial conidia with a round, blunt apical cell, and a rounded or barely notched, distinct, foot-like basal cell, with 5 approximately equidistant septa. I. Pigmented multiseptate sporodochial conidia. I–J. Multiseptate mature conidia with round to oval, rough-walled chlamydospore formation. K. Paired round to oval chlamydospores formed in hyphae. Bars: C = 1 mm; D–G = 20 µm; H–J = 15 µm; K = 10 µm

MycoBank MB834438

Typification: INDONESIA. RIAU: Pelalawan, *Acacia crassicarpa* plantation, isolated from the head (including mycangium) of a *Euwallacea similis* specimen, Mar 2019, *K.M.T. Lynn* (**holotype** PREM 62600). Ex-type strain CMW 54714 = PPRI 27971 = CBS 146885. GenBank: ITS-28S rDNA = MN954342; *TEF1-α* = MT009956; *RPB*2-1 = MT009916; *RPB*2-2 = MT009996.

Etymology: The name *mekan* is derived from the Bahasa Indonesia word "mekan" meaning eat or food. It reflects the relationship this fungus has with its beetle vector, *E. similis*, after a beetle was observed consuming this fungus.

Culture characteristics: Colony color on PDA white, grayish flax blue to grayish violet in dark, white to pale mouse gray darkening to purple state and rust after 1 mo in ambient daylight, occasionally with white, albino segments or streaks. Colony margin on PDA undulate, colony umbonate, occasionally raised. Reverse pigmentation yellowish white to fawn in dark, bay darkening to chestnut and blood red after 1 mo in ambient daylight. Odor absent. Rose exudates occasionally present. Colonies on PDA radial mycelial growth rates of average 2.46 mm/d at 15 C, 4.84 mm/d at 20 C, 5.89 mm/d at 25 C, 6.69 mm/d at 30 C, and 0.75 mm/d at 35 C in dark. Conidial pustules luteous to ochreous, produced on sporodochia on older cultures grown on PDA. Aerial mycelium sparse, or developed abundantly, loose to floccose, white to grayish/brown white. Chlamydospores formed abundantly in hyphae and mature conidia, mostly round to oval, intercalary or terminal, often single or paired, rarely clustered, ordinary hyaline, smooth, often rough-walled, 5–(6)–8–(10)–13 × 6–(7)–8–(9)–11 µm. Sclerotia absent. Sporulation on SNA abundant, particularly under UV light, retarded on PDA. Sporodochia formed sparsely on SNA, abundantly on PDA. Aerial conidiophores formed abundantly on SNA and PDA, often branching, erect or occasionally slightly curved, varying in length, thin-walled, tapering toward the base and slightly toward the apex, 63–(83)–133–(183)–232 × 2–(5)–5–(6)–8 µm, forming monophialides integrated in apices. Aerial phialides simple, subcylindrical, with discreet collarette. Aerial conidia (i) mostly oval, 2-celled oval to obovoid with truncated base, occasionally pyriform, 0–1(–2) septa, 8–(9)–12–(15)–29 × 3–(3)–4–(5)–5.5 µm; (ii) thick, curved with slight tapering toward the base, often with a round, blunt apical cell, and rounded basal cell, 0–3(–4)-septate, morphologically similar to long, oval-shaped sporodochial conidia. Sporodochial conidiophores thick, cylindrical, varying in length, occasionally branched, forming apical monophialides. Sporodochial phialides simple, subcylindrical, tube-shaped, with discreet collarette. Sporodochial conidia ordinarily hyaline, occasionally pigmented, thick, straight or occasionally slightly curved with discrete tapering toward the base, often with round, blunt apical cell, and rounded or barely notched, foot-like basal cell, 0–5(–6)-septate, formed on PDA and SNA, 20.5–(24)–31.5–(38.5)–45 × 4–(5)–6–(7)–9 µm. Obovoid to short-clavate or reniform, truncated base, slightly curved, with swollen, rounded apex, 0–1-septate, often formed together with multiseptate conidia on thick sporodochial conidiophores.

Habitat: Acacia crassicarpa plantations infested with ambrosia beetles in Riau, Indonesia.

Known distribution: Riau, Indonesia.

Additional specimens examined: INDONESIA. RIAU: Pelalawan, *Acacia crassicarpa* plantation, isolated from *A. crassicarpa* infested with *E. perbrevis* (TSHBa) and *E. similis*, Nov 2018, *K.M.T. Lynn*, **paratype** PREM 62601, ex-type culture CMW 53696 = PPRI 27956

= CBS 146886; ibid., isolated from the head (including mycangium) of a *Euwallacea similis* specimen, Nov 2018, *K.M.T. Lynn*, **paratype** PREM 62602, ex-type culture CMW 54717 = PPRI 27972 = CBS 146887.

Diagnosis: A distinguishing characteristic of this species is its multiseptate conidia that are slightly curved, elongate, and oval, and in which the septa appear consistently spaced from each other. The production of chlamydospores at both the apex and the base of single mature conidia is also a diagnostic feature. This species resides within clade B of the AFC. It is phylogenetically distinct from other previously described AFC species based on a maximum likelihood analysis using the *TEF1-α* gene region (SUPPLEMENTARY FIG. 3) and a multilocus analysis using three loci (ITS-28S rDNA, *TEF1-α*, and *RPB2*) (FIG. 3).

Fusarium variasi Lynn & I. Barnes, sp. nov. FIG. 7

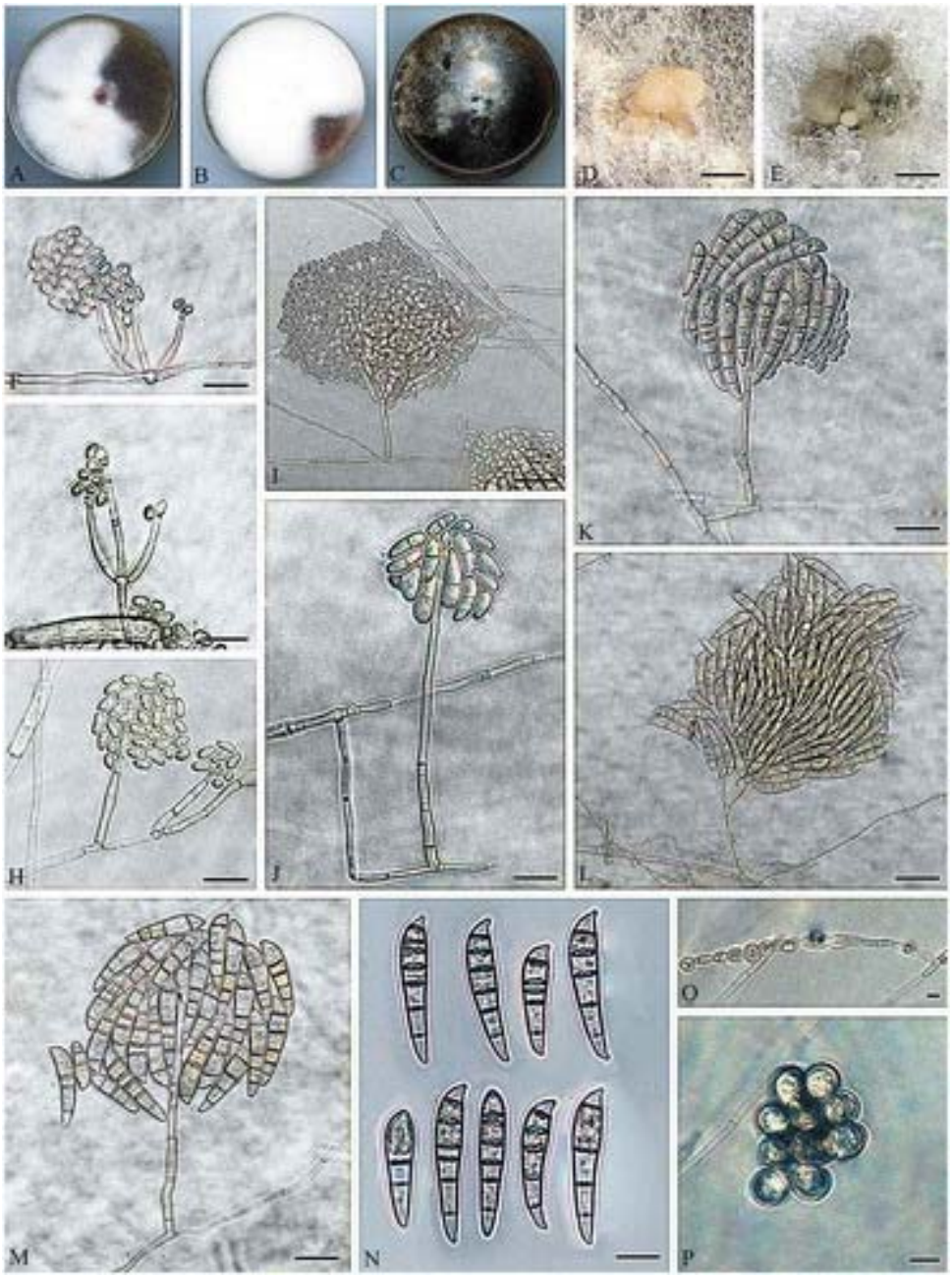

Figure 7. Morphological characteristics of *Fusarium variasi* on PDA and SNA (CMW 53734, CMW 53735, and CMW 54696). A–E, N. Morphology of *F. variasi* cultures grown on potato dextrose agar (PDA). O–P. Morphology of 14-d-old *F. variasi* cultures grown on synthetic low-nutrient agar (SNA). A–B. Colony morphology on PDA at 2 wk of CMW 53734 and CMW 54696, respectively. C–E. Luteous-ochreous to olive green conidial masses formed in culture on PDA after 1 mo. F–M. Simple to branched aerial conidiophores varying in length forming either (i) oval, obovoid or globose, nonseptated conidia, or (ii) 2-celled oval, short-clavate, curved, 0–1(2)-septate conidia, or (iii) clavate, slightly curved, apically papillated, 3–6-septate conidia. These conidia can form together on the same aerial conidiophore or separately. N. Multiseptate clavate sporodochial conidia with narrow papillate or occasionally rounded apical cell, and barely notched or distinct, foot-like basal cell, with 2–7 septa. O–P. Round to oval chlamydospores in chains or clustered formed in hyphae. Bars: D–E = 1 mm; F–M = 20 µm; N = 15 µm; O–P = 10 µm

MycoBank MB834439

Typification: INDONESIA. RIAU: Pelalawan, *Acacia crassicarpa* plantation, isolated from *A. crassicarpa* infested with *E. perbrevis* (TSHBa), Nov 2018, *K.M.T. Lynn* (**holotype** PREM 62595). Ex-type strain CMW 53734 = PPRI 27958 = CBS 146888. GenBank: ITS-28S rDNA = MN954356; *TEF1-α* = MT009953; *RPB*2-1 = MT009913; *RPB*2-2 = MT009993.

Etymology: The name *variasi* is derived from the Bahasa Indonesia word "variasi" meaning variation. It refers to the observed variation in the size and shape of the conidia.

Culture characteristics: Colony color on PDA white or livid purple to fawn in dark, white with livid purple to bay segments, darkening to dark brick or violate slate or black after 1 mo in ambient daylight. Colony margin on PDA entire, rarely filamentous, raised. Reverse pigmentation yellowish white to fawn in dark, white with rust to umber segments, occasionally entirely darkening to umber or black after 1 mo in ambient daylight. Odor absent. Occasional greenish yellow or red exudates present. Colonies on PDA radial mycelial growth rates of average 2.47 mm/d at 15 C, 3.49 mm/d at 20 C, 5.02 mm/d at 25 C, 6.79 mm/d at 30 C, and 0.36 mm/d at 35 C in dark. Conidial pustules produced on sporodochia, form on older cultures grown on PDA and SNA, luteous to ochreous or dull green to dark violet, particularly under UV light. Aerial mycelium sparse, or abundant, loose to floccose, white. Chlamydospores abundant in hyphae, mostly round to oval, intercalary or terminal, single, paired or in chains, often clustered, hyaline, smooth, often rough-walled, 6–(7)–8–(9)–11 × 6–(7)–8–(9)–11 µm. Sclerotia absent. Sporulation on SNA abundant, particularly under UV light, retarded on PDA. Sporodochia formed on SNA, abundant on PDA. Aerial conidiophores abundant on SNA and PDA, often branching, erect, varying in length, thin-walled and narrow, tapering toward the apex, 19–(40)–65–(90)–121 × 2–(3)–4–(5)–6 µm, forming monophialides integrated in apices. Aerial phialides simple, subcylindrical, with discreet collarette. Aerial conidia (i) mostly oval, obovoid with truncated base or globose, 0 septa, 4–(5)–6–(7)–9 × 2–(3)–4–(5)–5 µm; (ii) mostly 2-celled oval, short-clavate, curved, 0–1(2) septa, 13–(14)–17–(20)–25 × 4–(5)–6–(7)–9 µm; (iii) falcate to clavate, slightly curved, 3–5(–6)-septate, morphologically almost indistinguishable from falcate to clavate sporodochial conidia. Sporodochial conidiophores thick, cylindrical, often branched, forming apical monophialides. Sporodochial phialides simple, subcylindrical, tube-shaped, with discreet collarette. Sporodochial conidia ordinarily hyaline, falcate to clavate, thick, curved with tapering toward the base, with papillate, occasionally rounded apical cell, and barely notched or distinct, foot-like basal cell, 3–6(–7)-septate, formed on PDA and SNA, 44–(47)–52–(57)–64 × 8–(10)–12–(14)–15 µm. Short-clavate to oval, straight conidia, with rounded apex and occasionally truncate base, 0–1-septate, often formed together with multiseptate conidia borne on thick sporodochial conidiophores.

Habitat: Acacia crassicarpa plantations infested with ambrosia beetles in Riau, Indonesia.

Known distribution: Riau, Indonesia.

Additional specimens examined: INDONESIA. RIAU: Pelalawan, *Acacia crassicarpa* plantation, isolated from *A. crassicarpa* infested with *E. perbrevis* (TSHBa), Nov 2018, *K.M.T. Lynn*, **paratype** PREM 62596, ex-type culture CMW 53735 = PPRI 27959 = CBS 146889; ibid., Nov 2018, *K.M.T. Lynn*, **paratype** PREM 62597, ex-type culture CMW 54696 = PPRI 27968 = CBS 146890.

Diagnosis: This species is characterized by the highly variable size and shape of the aerial conidia and the clustering of these varied conidia on a single conidiophore. The conidia are small, obovoid, and clavate, multiseptate, and swollen, with papillate apical end or are shorter, clavate, septate and vary in shape. This species also produces abundant chlamydospores in clusters, unlike other species in the AFC. This species resides within clade A of the AFC. It is phylogenetically distinct from other previously described AFC species based on individual (SUPPLEMENTARY FIGS. 1–3) and combined analyses of the ITS-28S rDNA, *TEF1-α*, and *RPB2* gene regions (FIG. 3), respectively.

Note: This species might represent more than one taxon, based on the variation in the morphological characteristics and the strong bootstrap support for two branches in the phylogenetic trees. However, as no distinct morphological variation could be identified between the two discrete phylogenetic groups, we have chosen not to describe separate species before additional isolates can be collected to resolve the species boundaries more rigorously.

Fusarium warna Lynn & I. Barnes, sp. nov. FIG. 8

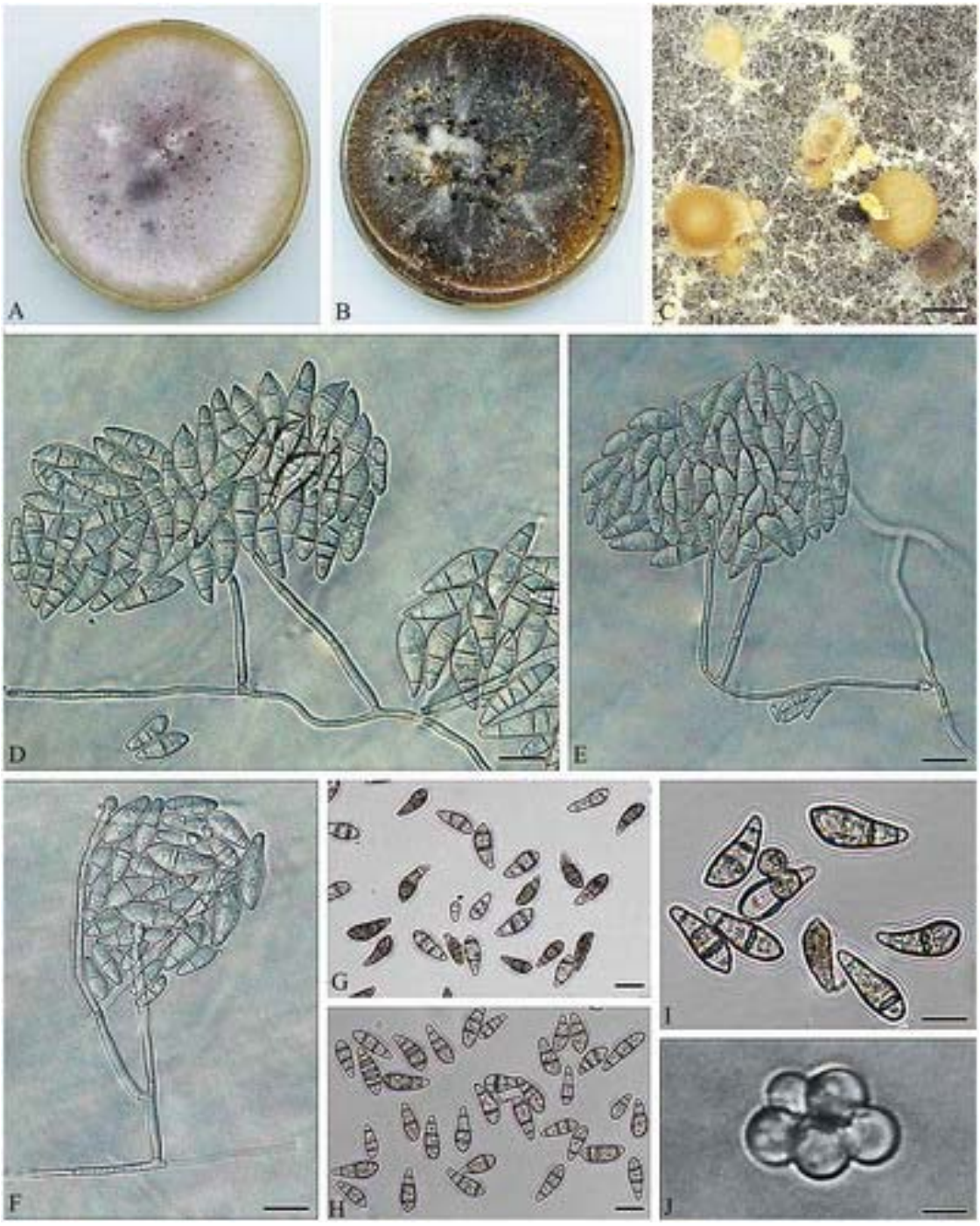

Figure 8. Morphological characteristics of *Fusarium warna* on PDA and SNA (CMW 54720, CMW 54724, and CMW 54726). A–C, G–I. Morphology of *F. warna* cultures grown on potato dextrose agar (PDA). D–F, J. Morphology of 14-d-old *F. warna* cultures grown on synthetic low-nutrient agar (SNA). A–B. Colony morphology on PDA at 2 wk. C. Luteous-ochreous to sepia conidial masses formed in culture on PDA after 1 mo. D–E. Simple to branched aerial conidiophores varying in length forming short obovoid conidia with truncated base with 0–3(–4) septa. G–H. Pigmented multiseptated short, clavate sporodochial conidia. I. Multiseptate conidia with round to oval, rough-walled chlamydospores. J. Round to oval chlamydospores, clustered, formed in hyphae. Bars: C = 1 mm; D–F = 15 µm; G-I = 10 µm; J = 5 µm

MycoBank MB834440

Typification: INDONESIA. RIAU: Pelalawan, *Acacia crassicarpa* plantation, isolated from the head (including mycangium) of a *Euwallacea perbrevis* (TSHBa) specimen, Mar 2019, *K.M.T. Lynn* (**holotype** PREM 62603). Ex-type strain CMW 54720 = PPRI 27974 = CBS 146891. GenBank: ITS-28S rDNA = MN954346; *TEF1-α* = MT009960; *RPB*2-1 = MT009920; *RPB*2-2 = MT010000.

Etymology: The name *warna* is derived from the Bahasa Indonesia word "warna" meaning color. It reflects the different colors of the fungus in culture, including the range of colors of the mycelium, the exudates produced, and the pigmented conidia.

Culture characteristics: Colony color on PDA white to livid purple to vinaceous purple, with white segments, to fawn on outer edges of culture in dark, lavender to violet or livid violet with white segments, darkening to livid vinaceous or dark vinaceous to dark purple with sepia edges after 1 mo in ambient daylight. Colony margin on PDA entire, flat to umbonate. Reverse pigmentation yellowish white to fawn in dark, pale vinaceous gray white with rust to umber darkening to dark brick after 1 mo in ambient daylight. Odor absent. Red to purple exudates often present. Colonies on PDA radial mycelial growth rates of an average of 2.17 mm/d at 15 C, 4.69 mm/d at 20 C, 6.83 mm/d at 25 C, 5.28 mm/d at 30 C, and 2.33 mm/d at 35 C in dark. Conidial pustules produced on sporodochia, form on older cultures grown on PDA, occasionally on SNA, are luteous to ochreous, or dull green to sepia. Aerial mycelium sparse, or abundant, loose to floccose, white to light purple. Chlamydospores sparse in hyphae and mature conidia, mostly round to oval, intercalary or terminal, single, paired, often clustered, ordinary hyaline, smooth, often rough-walled, 3.5–(4)–5–(6)–8 × 3–(4)–5–(6)–6.5 µm. Sclerotia absent. Sporulation on SNA abundant, particularly under UV light, retarded on PDA. Sporodochia formed on SNA, abundantly on PDA. Aerial conidiophores formed abundantly on SNA and PDA, often branching, slightly curved, varying in length, thick with no tapering toward the apex, 40–(57)–78–(99)–144 × 3–(3)–4–(5)–7 µm, forming monophialides integrated in apices. Aerial phialides simple, subcylindrical, with discreet collarette. Aerial conidia (i) mostly obovoid with truncated base, oval, or short-clavate, rarely curved, 0–3(–4) septa, 12–(14)–17–(20)–25 × 4–(6)–7–(8)–10 µm; (ii) clavate, straight, with bulging apical end and prominent tapering toward the base, 1–5(–7)-septate, morphologically almost indistinguishable from short-clavate sporodochial conidia. Sporodochial conidiophores thick, cylindrical, often branched, forming apical monophialides. Sporodochial phialides simple, subcylindrical, tube-shaped, with discreet collarette. Sporodochial conidia ordinarily hyaline or pigmented, thick, short-clavate, papillate or rounded, swollen apical cell, tapering toward the base, indistinct, foot-like or rounded basal cell, 1–4(–6)-septate, formed on PDA and SNA, 27.5–(30)–32–(34)–37.5 × 10–(12)–13–(14)–15 µm. Short-clavate to oval, straight conidia, with rounded apex and occasionally truncate base, nonseptated, often formed together with multiseptate conidia borne on thick sporodochial conidiophores.

Habitat: Acacia crassicarpa plantations infested with ambrosia beetles in Riau, Indonesia.

Known distribution: Riau, Indonesia.

Additional specimens examined: INDONESIA. RIAU: Pelalawan, *Acacia crassicarpa* plantation, isolated from the head (including mycangium) of a *Euwallacea perbrevis* (TSHBa) specimen, Mar 2019, *K.M.T. Lynn*, **paratype** PREM 62605, ex-type culture CMW

54724 = PPRI 27976 = CBS 146892; ibid., Mar 2019, *K.M.T. Lynn*, **paratype** PREM 62606, ex-type culture CMW 54726 = PPRI 27977 = CBS 146893.

Diagnosis: This species is characterized by multiseptate, thick, short, papillated, spindle-shaped sporodochial conidia that taper toward the base. The production of smaller chlamydospores compared with other species in the AFC is an additional diagnostic feature. This species resides within clade B of the AFC. It is phylogenetically distinct from other previously described AFC species based on a maximum likelihood analysis using the *RPB2* gene region (SUPPLEMENTARY FIG. 1) and a multilocus analysis using three loci (ITS-28S rDNA, *TEF1-α*, and *RPB2*) (FIG. 3).

Beetle-fungus associations.—

A nonexclusive relationship appears to exist between the ambrosia beetles *E. perbrevis* and *E. similis* and their *Fusarium* mutalists (Table 1). Table 1 depicts data regarding cultures isolated from the beetle mycangia only. *Fusarium akasia* (AF-20) was isolated from the mycangia of *E. similis* and *E. perbrevis* specimens; *F. awan* and *F. mekan* (AF-21) were recovered from the mycangia of *E. similis* specimens; *F. variasi* (AF-22) was recovered from a gallery harboring either *E. similis* or *E. perbrevis* larvae; and *F. warna* (AF-23) was isolated from the mycangia of *E. perbrevis* specimens. Additionally, *F. rekanum*, a previously identified associate of *E. perbrevis* (Lynn et al. 2020), was also obtained from mycangia of *E. similis* specimens in this study.

Table 1. Summarized data of *Fusarium* spp. isolated from the mycangia of two *Euwallacea* beetle species

Fusarium species based on combined analysis	Total number of isolates from mycangia[a]	Beetle vectors based on morphology	Confirmed *Euwallacea* spp. vector based on *COI* sequence data[b]
F. rekanum (AF-19)	51	*Euwallacea perbrevis*	30
		Euwallacea similis	11
F. akasia (AF-20)	21	*E. perbrevis*	10
		E. similis	1
F. awan	34	*E. similis*	23
F. mekan (AF-21)	3	*E. similis*	3
F. warna (AF-23)	4	*E. perbrevis*	4

Note. Although 114 *Euwallacea* beetles were collected, the *COI* gene region did not successfully amplify in all 114 specimens. Therefore, only selected fungal isolates that could be correctly correlated to a beetle vector that had *COI* sequence data, were used to infer beetle fungi fidelity.
[a]Identity of isolates confirmed with both morphological and phylogenetic data.
[b]Only a subset of these isolates were incorporated into the phylogenetic tree depicted in FIG. 3, to ensure legibility.

The prevalence of the different *Fusarium* associates isolated from the mycangia of their corresponding *Euwallacea* spp. beetle hosts also varied (Table 1). All *Fusarium* isolates were consistently identified using morphological observations and phylogenetic analyses as described above. However, the identity of several of the corresponding beetle specimens processed could not be successfully confirmed with sequence data. Consequently, information regarding *Fusarium* mutualist fidelity was restricted to isolates gathered from the mycangia of beetle specimens that could be correctly identified based on both morphological and sequence data.

Fusarium rekanum (30 isolates) was the most abundant AFC member isolated from the mycangia of *E. perbrevis* specimens, followed by *F. akasia* (10 isolates) and *F. warna* (4 isolates). Similarly, *F. awan* (23 isolates) was the mutualist most often isolated from the mycangia of *E. similis* specimens, followed by *F. rekanum* (11 isolates), *F. mekan* (2 isolates), and *F. akasia* (1 isolate). The one *F. akasia* isolate was recovered from the mycangium of an *E. similis* specimen coinhabiting a gallery occupied by *E. perbrevis*

specimens. Mycangial isolations from these *E. perbrevis* specimens also yielded *F. akasia* isolates.

Overall, regardless of beetle mutualist, *Fusarium rekanum* was the most common *Fusarium* species isolated from both mycangia and brood galleries. This was closely followed by *F. awan* and *F. akasia*. The remaining three *Fusarium* species were less prevalent, with only five isolates of *F. mekan*, four isolates of *F. warna*, and three isolates *F. variasi* recovered. The abundance of the novel *Fusarium* species also correlated to their distribution across the five plantation compartments. *Fusarium rekanum* was collected from all five compartments, *F. awan* was collected from four compartments, and *F. akasia* from three compartments. *Fusarium mekan, F. warna*, and *F. variasi* were collected from only one compartment each.

DISCUSSION

This study investigated the identity and specificity of fungal mutualists of the two most common ambrosia beetles on *Acacia crassicarpa* plantations in Riau, Indonesia. The ambrosia beetles were identified as *E. perbrevis* and *E. similis*. Five of the *Fusarium* mutualists of these beetles were shown to be novel species, including *F. akasia* (AF-20), *F. awan, F. mekan* (AF-21), *F. variasi* (AF-22), and *F. warna* (AF-23). Although these two *Euwallacea* species have been shown to carry several *Fusarium* mutualists, most of the novel *Fusarium* mutualists identified in this study were isolated from only one of the two beetle species.

Both *E. similis* and *E. perbrevis* were commonly found infesting the same *A. crassicarpa* tree, and they were occasionally also found coinhabiting a single brood gallery. However, *E. similis* was never found infesting a host where *E. perbrevis* was not also present. Therefore, *E. similis* appears to be a secondary invader requiring a tree to be weakened or already infested before colonization can occur and thus behaving in a manner typical of ambrosia beetle ecology. This supports the findings of Lynn at al. (2020) and Balasundaran and Sankaran (1991) where *E. similis* was also reported to usually infest only stressed or dying trees.

Phylogenetic analyses of the *COI* gene region showed a high level of intraspecific genetic diversity in both identified *Euwallacea* spp. The *COI* gene region is known to have high levels of intraspecific variation when distinguishing species in the Xyleborini (Jordal and Kambestad 2014). Consequently, it is not possible to determine whether the *COI* data presented in this study, showing distinct divergence between the four novel *E. similis* haplotypes, provide indication of cryptic speciation. Alternatively, this might simply reflect genetic diversity within the species due to the intraspecific *COI* variation (Jordal and Kambestad 2014).

Six *Fusarium* species were found mutualistically associated with the two *Euwallacea* species encountered in this study. Five of these were novel, four of which reside in the AFC clade (Kasson et al. 2013), and one grouped just outside the AFC clade but still resides within the greater *Fusarium solani* species complex (FSSC). These novel species were identified based on phenotypic and morphological characters (Gadd and Loos 1947; Freeman et al. 2013; Aoki et al. 2018, 2019; Na et al. 2018). *Fusarium akasia* (AF-20), *F. mekan* (AF-21), and *F. warna* (AF-23) reside in clade B of the AFC. *Fusarium variasi* (AF-22) grouped with AF-8 and AF-9 in clade A of the AFC, and *F. awan* formed a sister clade with *F. lichenicola* (NRRL 32434). Interestingly, the species that have been formally described and that reside in

clade B of the AFC have been found to almost exclusively produce clavate multiseptate sporodochial conidia, or a combination of fusiform and clavate multiseptate sporodochial conidia. This is in contrast to the predominately fusiform conidia found by *Fusarium* species in clade A (Kasson et al. 2013; Aoki et al. 2018). A shift from producing predominately fusiform to apically swollen clavate sporodochial conidia is believed to be an evolutionary adaptation of these fungi to their symbiotic *Euwallacea* spp. (Kasson et al. 2013). However, two of the described species in this study did not conform to this pattern. *Fusarium mekan* (AF-21) in clade B, in addition to the undescribed AF-6 species, produced discrete fusiform conidia rather than clavate conidia. Similarly, *F. variasi* (AF-22) in clade A produced masses of clavate conidia rather than fusiform conidia.

Euwallacea perbrevis has now been reported to be associated with eight members of the AFC, two of which are novel species described in the present study. Five of these associates were first collected from countries other than Indonesia. These are AF-1 from India/Sri Lanka and AF-13, AF-14, AF-17, and AF-18 from Taiwan and were all isolated from tree species other than *A. crassicarpa* (Carrillo et al. 2019). None of these five previously isolated AFC species were isolated from the mycangia of *E. similis* or *E. perbrevis*, or from their corresponding brood galleries such as those analyzed in the present study. The absence of these other AFC associates from the beetle specimens analyzed in the present study could reflect the geographic origins, plant hosts, and different haplotypes of the beetle vectors.

In comparison with other *Euwallacea* species, very little research has been conducted on the fungal mutualists of *E. similis*. A previous study by Balasundaran and Sankaran (1991) suggested that *F. solani*, externally vectored by *E. similis*, was the causal agent of the canker and dieback disease of teak (*Tectona grandis*) in Kerala, India. However, the *Fusarium solani* complex accommodates many species that vary in aggressiveness and ecology (Sandoval-Denis et al. 2019; Geiser et al. 2020). The taxonomic boundaries of this complex have changed drastically since 1991, and until recently its species diversity has been largely understudied (Sandoval-Denis et al. 2019; Geiser et al. 2020). Thus, it is possible that the species identified by Balasundaran and Sankaran (1991) was a cryptic species in the *Fusarium solani* complex. Regardless of this fact, based on the data available, *Fusarium solani* was never isolated from the mycangia or brood galleries of *E. similis* specimens investigated in this study. Rather, four novel *Fusarium* species were associated with the beetle, all of which appeared to be nutritional mutualists.

Results of this study revealed further evidence for a nonspecific association of these beetle species with AFC members and is consistent with previous findings (O'Donnell et al. 2015; Lin et al. 2017; Carrillo et al. 2019; Skelton et al. 2019). Although there appeared to be little specificity between these *Euwallacea* spp. and their *Fusarium* associates, some vector preference in this symbiosis was suggested by the different prevalences of the *Fusarium* species isolated from the two *Euwallacea* species, as depicted in Table 1. This could be a consequence of the sampling strategy used, or that the most abundant *Fusarium* species isolated are better suited to enable their respective beetle vectors to colonize *A. crassicarpa* compared with other AFC members or *Fusarium* mutualists (Klepzig et al. 2009; Six et al. 2011). The preoral mycangia of these two *Euwallacea* species could also be imposing a selective pressure, favoring the fidelity of certain *Fusarium* mutualists over others (Skelton et al. 2019). Alternatively, the association of the *Fusarium* spp. with their *Euwallacea* beetle vectors could also be influenced by prevailing temperatures in the areas where the beetles are found (Six et al. 2011). For example, Riau, Indonesia, the location of the present study, has a

relatively high average annual temperature that appears to be consistent with the optimal temperatures for growth of *F. rekanum* and *F. awan.*

When studied in their non-native ranges, members of the AFC appear to be relatively host specific (Freeman et al. 2013; Na et al. 2018). However, in their native range, these fungi are apparently much more promiscuous (Carrillo et al. 2019), as was also seen for the five new species described in the present study. These results highlight the importance of studying these ambrosia beetle–fungus mutualisms in their native habitats, where "bottleneck" events have not altered the diversity of the fungal mutualists.

The results of this study are consistent with previous investigations considering the fidelity of other ambrosia beetle–fungus mutualisms in the Hypocreales and Microascales (O'Donnell et al. 2015; Lin et al. 2017; Carrillo et al. 2019; Mayers et al. 2020). Ambrosia fungi in the Microascales and Hypocreales (O'Donnell et al. 2015; Carrillo et al. 2019; Skelton et al. 2019) have been shown to have a broad symbiont specificity, in which closely related beetle species can switch between fungal mutualists (Lin et al. 2017; Carrillo et al. 2019; Lehenberger et al. 2019; Mayers et al. 2020). This is most likely a result of coevolution between these fungal mutualists and their beetle vectors, resulting in mycangia designed to aid in the horizontal transmission and growth of core fungal mutualists, but also to allow the same conditions for closely related fungal species (Skelton et al. 2019; Mayers et al. 2020). Thus, although varying degrees of ambrosial fungal mutualist specificity appears to exist, fungal species-level coevolution does not occur (Mayers et al. 2020).

Results of this study suggest that the five new *Fusarium* species are cultivated by the two *Euwallacea* ambrosia beetles from which they were isolated (Table 1) and act as nutritional mutualists. This will, however, need to be tested with diet experiments similar to those conducted by Freeman et al. (2013) and Carrillo et al. (2020). Future studies should also consider the survival of these beetle species on all the various AFC members, as suggested by Carrillo et al. (2020).

Although most fungus-farming *Euwallacea* spp. have no significant economic consequences (Hulcr and Stelinski 2017), they have the potential to cultivate the symbionts of other closely related beetle species that are economically important (Gebhardt et al. 2004; O'Donnell et al. 2015). The potential to switch symbionts could result in the emergence of more destructive and economically damaging *Euwallacea-Fusarium* associations. These emerging issues regarding the biology and importance of *Euwallacea* spp. are gaining increasing attention (Hulcr et al. 2020) and will need to be studied more thoroughly in the future.

ACKNOWLEDGMENTS

We thank Wilma Nel and members of the Asia Pacific Resources International Holdings Ltd. (APRIL) Group, Royal Golden Eagle (RGE), Indonesia, particularly Pantun David Mangatas Lumban Gaol, Hengki Marantika, and Wagner de Souza Tavares and his team, for their technical assistance. We are also grateful to Dr. Andrew J. Johnson and Dr. You Li from the University of Florida, Gainesville (UF) Forest Entomology Laboratory, who kindly provided the photographs for FIG. 1A and B. We thank Felipe Balocchi Schalchli for suggestions during the revision of an earlier draft of the manuscript. We also thank the two reviewers for their valuable inputs, which both contributed to and improved the manuscript.

Funding
This study was initiated through the bilateral agreement between the Forestry and Agricultural Biotechnology Institute (FABI), University of Pretoria, and the APRIL Group, RGE, Indonesia. We acknowledge funding from the RGE-FABI Tree Health Programme and the National Research Foundation (NRF, SFH170527234109), South Africa.

LITERATURE CITED

Aoki T, Kasson M, Berger MC, Freeman S, Geiser DM, O'Donnell K. 2018. *Fusarium oligoseptatum* sp. nov., a mycosymbiont of the ambrosia beetle *Euwallacea validus* in the Eastern U.S. and typification of *F. ambrosium*. Fungal Systematics and Evolution 1:23–39.

Aoki T, O'Donnell K, Scandiani MM. 2005. Sudden death syndrome of soybean in South America is caused by four species of *Fusarium: Fusarium brasiliense* sp. nov., *F. cuneirostrum* sp. nov., *F. tucumaniae*, and *F. virguliforme*. Mycoscience 46:162–183.

Aoki T, Smith JA, Kasson MT, Freeman S, Geiser D, Andrew D, O'Donnell G, O'Donnell K. 2019. Three novel Ambrosia *Fusarium* Clade species producing clavate macroconidia known (*F. floridanum* and *F. obliquiseptatum*) or predicted (*F. tuaranense*) to be farmed by *Euwallacea* spp. (Coleoptera: Scolytinae) on woody hosts. Mycologia 111:919–935.

Beaver RA. 1989. Insect–Fungus relationships in the bark and ambrosia beetles. In: Wilding N, Collins NM, Hammond PM, Webber JF, eds. Insect-fungus interactions. London, UK: Academic Press. p. 121–143.

Bumrungsri S, Beaver R, Phongpaichit S, Sittichaya W. 2008. The infestation by an exotic ambrosia beetle, *Euplatypus parallelus* (F.) (Coleoptera: Curculionidae: Platypodinae) of Angsana trees (*Pterocarpus indicus* Willd.) in southern Thailand. Songklanakarin Journal of Science and Technology 30:579–582.

Carrillo D, Cruz LF, Kendra PE, Narvaez TI, Montgomery WS, Monterroso A, De Grave C, Cooperband MF. 2016. Distribution, pest status and fungal associates of *Euwallacea* nr. *fornicatus* in Florida avocado groves. Insects 7:1–11.

Carrillo JD, Dodge C, Stouthamer R, Eskalen A. 2020. Fungal symbionts of the polyphagous and Kuroshio shot hole borers (Coleoptera: Scolytinae, *Euwallacea* spp.) in California can support both ambrosia beetle systems on artificial media. Symbiosis 80:1–14.

Carrillo JD, Rugman-Jones PF, Husein D, Stajich JE, Kasson MT, Carrillo D, Stouthamer R, Eskalen A. 2019. Members of the *Euwallacea fornicatus* species complex exhibit promiscuous mutualism with ambrosia fungi in Taiwan. Fungal Genetics and Biology 133:1–12.

Cognato AI, Hoebeke ER, Kajimura H, Smith SM. 2015. History of the exotic ambrosia beetles *Euwallacea interjectus* and *Euwallacea validus* (Coleoptera: Curculionidae: Xyleborini) in the United States. Journal of Economic Entomology 108:1129–1135.

Eatough Jones M, Paine TD. 2017. Differences among avocado cultivars in susceptibility to polyphagous shot hole borer (*Euwallacea* spec.). Entomologia Experimentalis et Applicata 163:296–304.

Eskalen A, Stouthamer R, Lynch SC, Rugman-Jones PF, Twizeyimana M, Gonzalez A, Thibault T. 2013. Host range of Fusarium dieback and its ambrosia beetle (Coleoptera: Scolytinae) vector in southern California. Plant Disease 97:938–951.

Folmer O, Black M, Hoeh W, Lutz R, Vrijenhoek R. 1994. DNA primers for amplification of mitochondrial cytochrome c oxidase subunit I from diverse metazoan invertebrates. Molecular Marine Biology and Biotechnology 3:294–299.

Fraedrich SW, Harrington TC, Best GS. 2015. *Xyleborus glabratus* attacks and systemic colonization by *Raffaelea lauricola* associated with dieback of *Cinnamomum camphora* in the southeastern United States. Forest Pathology 45:60–70.

Fraedrich SW, Harrington TC, Rabaglia RJ, Ulyshen MD, Mayfield AE, Hanula JL, Eickwort JM, Miller DR. 2008. A fungal symbiont of the redbay ambrosia beetle causes a lethal wilt in redbay and other Lauraceae in the southeastern United States. Plant Disease 92:215–224.

Francke-Grosmann H. 1967. Ectosymbiosis in wood-inhabiting insects. In: Henry S, ed. Symbiosis. New York: Academic Press. p. 141–206.

Freeman S, Sharon M, Dori-Bachash M, Maymon M, Belausov E, Maoz Y, Margalit O, Protasov A, Mendel Z. 2016. Symbiotic association of three fungal species throughout the life cycle of the ambrosia beetle *Euwallacea* nr. fornicatus. Symbiosis 68:115–128.

Freeman S, Sharon M, Maymon M, Mendel Z, Protasov A, Aoki T, Eskalen A, O'Donnell K. 2013. *Fusarium euwallaceae* sp. nov.—a symbiotic fungus of *Euwallacea* sp., an invasive ambrosia beetle in Israel and California. Mycologia 105:1595–1606.

Gadd CH, Loos CA. 1947. The ambrosia fungus of *Xyleborus fornicatus* Eich. Transactions of the British Mycological Society 31:13–19.

Gebhardt H, Begerow D, Oberwinkler F. 2004. Identification of the ambrosia fungus of *Xyleborus monographus* and *X. dryographus* (Coleoptera: Curculionidae, Scolytinae). Mycological Progress 3:95–102.

Geiser DM, Al-Hatmi A, Aoki T, Arie T, Balmas V, Barnes I, Bergstrom GC, Bhattacharyya MKK, Blomquist CL, Bowden R, Brankovics B, Brown DW, Burgess LW, Bushley K, Busman M, Cano-Lira JF, Carrillo JD, Chang HX, Chen CY, Chen W, Chilvers MI, Chulze SN, Coleman JJ, Cuomo CA, de Beer ZW, de Hoog GS, Del Castillo-Múnera J, Del Ponte E, Diéguez-Uribeondo J, Di Pietro A, Edel-Hermann V, Elmer WH, Epstein L, Eskalen A, Esposto MC, Everts KL, Fernández-Pavía SP, da Silva GF, Foroud NA, Fourie G, Frandsen RJN, Freeman S, Freitag M, Frenkel O, Fuller KK, Gagkaeva T, Gardiner DM, Glenn AE, Gold S, Gordon T, Gregory NF, Gryzenhout M, Guarro J, Gugino B, Gutiérrez S, Hammond-Kosack K, Harris LJ, Homa M, Hong CF, Hornok L, Huang JW, Ilkit M, Jacobs A, Jacobs K, Jiang C, Jimenez-Gasco MDM, Kang S, Kasson MT, Kazan K, Kennell JC, Kim H, Kistler HC, Kuldau GA, Kulik T, Kurzai O, Laraba I, Laurence MH, Lee TY, Lee YW, Lee YH, Leslie JF, Liew ECY, Lofton LW, Logrieco A, Sánchez López-Berges M, Luque AG, Lysøe E, Ma LJ, Marra RE, Martin FN, May SR, McCormick S, McGee CT, Meis JF, Migheli Q, Mohamed Nor NMI, Monod M, Moretti A, Mostert D, Mulé G, Munaut F, Munkvold GP, Nicholson P, Nucci M, O'Donnell K, Pasquali M, Pfenning LH, Prigitano A, Proctor R, Ranque S, Rehner S, Rep M, Rodríguez-Alvarado G, Rose LJ, Roth MG, Ruiz-Roldán C,

Saleh AA, Salleh B, Sang H, Scandiani M, Scauflaire J, Schmale D, 3rd, Short DP, Šišić A, Smith J, Smyth CW, Son H, Spahr E, Stajich JE, Steenkamp E, Steinberg C, Subramaniam R, Suga H, Summerell BA, Susca A, Swett CL, Toomajian C, Torres-Cruz TJ, Tortorano AM, Urban M, Vaillancourt LJ, Vallad GE, van der Lee T, Vanderpool D, van Diepeningen AD, Vaughan M, Venter E, Vermeulen M, Verweij PE, Viljoen A, Waalwijk C, Wallace EC, Walther G, Wang J, Ward T, Wickes B, Wiederhold NP, Wingfield MJ, Wood AKM, Xu JR, Yang XB, Yli-Matilla T, Yun SH, Zakaria L, Zhang H, Zhang N, Zhang S, Zhang X. 2020. Phylogenomic analysis of a 55.1 kb 19-gene dataset resolves a monophyletic *Fusarium* that includes the *Fusarium solani* species complex. Phytopathology, doi:10.1094/phyto-08-20-0330-le

Gomez DF, Skelton J, Steininger MS, Stouthamer R, Rugman-jones P, Sittichaya W, Rabaglia RJ, Hulcr J. 2018. Species delineation within the *Euwallacea fornicatus* (Coleoptera : Curculionidae) complex revealed by morphometric and phylogenetic analyses. Insect Systematics and Diversity 2:1–11.

Harrington TC. 2005. Ecology and evolution of mycophagous bark beetles and their fungal partners. In: Vega FE, Blackwell M, eds. Ecological and evolutionary advances in insect-fungal associations. Oxford, UK: Oxford University Press. p. 257–291.

Hughes MA, Riggins JJ, Koch FH, Cognato AI, Anderson C, Formby JP, Dreaden TJ, Ploetz RC, Smith JA. 2017. No rest for the laurels: symbiotic invaders cause unprecedented damage to southern USA forests. Biological Invasions 19:2143–2157.

Hulcr J, Barnes I, de Beer ZW, Duong TA, Gazis R, Johnson AJ, Jusino MA, Kasson MT, Li Y, Lynch S, Mayers C, Musvuugwa T, Roets F, Seltmann K, Six D, Vanderpool D, Villari C. 2020. Bark beetle mycobiome: collaboratively defined research priorities on a widespread insect-fungus symbiosis. Symbiosis 81:101–113.

Hulcr J, Dunn RR. 2011. The sudden emergence of pathogenicity in insect-fungus symbioses threatens naive forest ecosystems. Proceedings of the Royal Society B: Biological Sciences 278:2866–2873.

Hulcr J, Stelinski LL. 2017. The ambrosia symbiosis: from evolutionary ecology to practical management. Annual Review of Entomology 62:285–303.

Jacobs K, Bergdahl DR, Wingfield MJ, Halik S, Seifert KA, Bright DE, Wingfield BD. 2004. *Leptographium wingfieldii* introduced into North America and found associated with exotic *Tomicus piniperda* and native bark beetles. Mycological Research 108:411–418.

Jordal BH, Kambestad M. 2014. DNA barcoding of bark and ambrosia beetles reveals excessive NUMTs and consistent east-west divergence across Palearctic forests. Molecular Ecology Resources 14:7–17.

Kasson MT, O'Donnell K, Rooney AP, Sink S, Ploetz RC, Ploetz JN, Konkol JL, Carrillo D, Freeman S, Mendel Z, et al. 2013. An inordinate fondness for *Fusarium*: phylogenetic diversity of *fusaria* cultivated by ambrosia beetles in the genus *Euwallacea* on avocado and other plant hosts. Fungal Genetics and Biology 56:147–157.

Katoh K, Standley DM. 2013. MAFFT multiple sequence alignment software version 7: improvements in performance and usability. Molecular Biology and Evolution 30:772–780.

Klepzig KD, Adams AS, Handelsman J, Raffa KF. 2009. Symbioses: a key driver of insect physiological processes, ecological interactions, evolutionary diversification, and impacts on humans. Environmental Entomology 38:67–77.

Kück P, Longo GC. 2014. FASconCAT-G: extensive functions for multiple sequence alignment preparations concerning phylogenetic studies. Frontiers in Zoology 11:1–8.

Kumar S, Stecher G, Tamura K. 2016. MEGA7: Molecular Evolutionary Genetics Analysis version 7.0 for bigger datasets. Molecular Biology and Evolution 33:1870–1874.

Kurtzman CP, Robnett CJ. 1997. Identification of clinically important ascomycetous yeasts based on nucleotide divergence in the 5' end of the large-subunit (26S) ribosomal DNA gene. Journal of Clinical Microbiology 35:1216–1223.

Lehenberger M, Biedermann PHW, Benz JP. 2019. Molecular identification and enzymatic profiling of *Trypodendron* (Curculionidae: Xyloterini) ambrosia beetle-associated fungi of the genus *Phialophoropsis* (Microascales: Ceratocystidaceae). Fungal Ecology 38:89–97.

Leslie JF, Summerell BA. 2006. The Fusarium laboratory manual. Victoria, Australia: Blackwell. 387 p.

Lin YT, Shih HH, Hulcr J, Lin CS, Lu SS, Chen CY. 2017. *Ambrosiella* in Taiwan including one new species. Mycoscience 58:242–252.

Lynch SC, Twizeyimana M, Mayorquin JS, Wang DH, Na F, Kayim M, Kasson MT, Thu PQ, Bateman C, Rugman-Jones P, Hulcr J, Stouthamer R, Eskalen A. 2016. Identification, pathogenicity and abundance of *Paracremonium pembeum* sp. nov. and *Graphium euwallaceae* sp. nov.—two newly discovered mycangial associates of the polyphagous shot hole borer (*Euwallacea* sp.) in California. Mycologia. 108:313–329.

Lynn KMT, Wingfield MJ, Durán A, Marincowitz S, Oliveira LSS, de Beer ZW, Barnes I. 2020. *Euwallacea perbrevis* (Coleoptera: Curculionidae: Scolytinae), a confirmed pest on *Acacia crassicarpa* in Riau, Indonesia, and a new fungal symbiont; *Fusarium rekanum*. Antonie van Leeuwenhoek 8:1–21.

Mayers CG, Harrington TC, Masuya H, Jordal BH, McNew DL, Shih H-H, Roets F, Kietzka GJ. 2020. Patterns of coevolution between ambrosia beetle mycangia and the Ceratocystidaceae, with five new fungal genera and seven new species. Persoonia 44:41–66.

Mendel Z, Protasov A, Sharon M, Zveibil A, Yehuda S Ben, O'Donnell K, Rabaglia R, Wysoki M, Freeman S. 2012. An Asian ambrosia beetle *Euwallacea fornicatus* and its novel symbiotic fungus *Fusarium* sp. pose a serious threat to the Israeli avocado industry. Phytoparasitica 40:235–238.

Miller MA, Pfeiffer W, Schwartz T. 2010. Creating the CIPRES science gateway for inference of large phylogenetic trees. In: 2010 Gateway Computing Environments Workshop. New Orleans, LA, 2010. p. 1–8. doi:10.1109/GCE.2010.5676129

Na F, Carrillo JD, Mayorquin JS, Ndinga-Muniania C, Stajich JE, Stouthamer R, Huang Y-T, Lin Y-T, Chen C-Y, Eskalen A. 2018. Two novel fungal symbionts *Fusarium kuroshium* sp. nov. and *Graphium kuroshium* sp. nov. of Kuroshio shot hole borer (*Euwallacea* sp. nr. *fornicatus*) cause Fusarium Dieback on woody host species in California. Plant Disease 102:1154–1164.

Norris DM, Baker JM. 1968. A minimal nutritional substrate required by *Fusarium solani* to fulfill its mutualistic relationship with *Xyleborus ferrugineus*. Annals of the Entomological Society of America 61:1473–1475.

O'Donnell K, Cigelnik E. 1997. Two divergent intragenomic rDNA ITS2 types within a monophyletic lineage of the fungus *Fusarium* are nonorthologous. Molecular Phylogenetics and Evolution 7:103–116.

O'Donnell K, Kistler HC, Cigelnik E, Ploetz RC. 1998. Multiple evolutionary origins of the fungus causing Panama disease of banana: concordant evidence from nuclear and mitochondrial gene genealogies. Proceedings of the National Academy of Sciences of the United States of America 95:2044–2049.

O'Donnell K, Libeskind-Hadas R, Hulcr J, Bateman C, Kasson MT, Ploetz RC, Konkol JL, Ploetz JN, Carrillo D, Campbell A, Duncan RE, Liyanage PNH, Eskalen A, Lynch SC, Geiser DM, Freeman S, Mendel Z, Sharon M, Aoki T, Cossé AA, Rooney AP. 2016. Invasive Asian *Fusarium–Euwallacea* ambrosia beetle mutualists pose a serious threat to forests, urban landscapes and the avocado industry. Phytoparasitica 44:435–442.

O'Donnell K, Sarver BAJ, Brandt M, Chang DC, Noble-Wang J, Park BJ, Sutton DA, Benjamin L, Lindsley M, Padhye A, Geiser DM, Ward TJ. 2007. Phylogenetic diversity and microsphere array-based genotyping of human pathogenic *fusaria*, including isolates from the multistate contact lens-associated U.S. keratitis outbreaks of 2005 and 2006. Journal of Clinical Microbiology 45:2235–2248.

O'Donnell K, Sink S, Libeskind-Hadas R, Hulcr J, Kasson MT, Ploetz RC, Konkol JL, Ploetz JN, Carrillo D, Campbell A, Duncan RE, Liyanage PNH, Eskalen A, Na F, Geiser DM, Bateman C, Freeman S, Mendel Z, Sharon M, Aoki T, Cossé AA, Rooney AP. 2015. Discordant phylogenies suggest repeated host shifts in the *Fusarium-Euwallacea* ambrosia beetle mutualism. Fungal Genetics and Biology 82:277–290.

O'Donnell K, Sutton DA, Rinaldi MG, Sarver BAJ, Balajee SA, Schroers HJ, Summerbell RC, Robert VARG, Crous PW, Zhang N, Aoki T, Jung K, Park J, Lee YH, Kang S, Park B, Geiser DM. 2010. Internet-accessible DNA sequence database for identifying *fusaria* from human and animal infections. Journal of Clinical Microbiology 48:3708–3718.

Paap T, de Beer W, Migliorini D, Nel WJ, Wingfield MJ. 2018. The polyphagous shot hole borer (PSHB) and its fungal symbiont *Fusarium euwallaceae*: a new invasion in South Africa. Australasian Plant Pathology 47:231–237.

Ploetz RC, Hulcr J, Wingfield MJ, de Beer WZ. 2013. Destructive tree diseases associated with ambrosia and bark beetles: black swan events in tree pathology. Plant Disease 95:856–872.

Sandoval-Denis M, Lombard L, Crous PW. 2019. Back to the roots: a reappraisal of *Neocosmospora*. Persoonia 43:90–185.

Six DL, Poulsen M, Hansen AK, Wingfield MJ, Roux J, Eggleton P, Slippers B, Paine TD. 2011. Anthropogenic effects on interaction outcomes: examples from insect-microbial symbioses in forest and savanna ecosystems. Symbiosis 53:101–121.

Skelton J, Johnson AJ, Jusino MA, Bateman CC, Li Y, Hulcr J. 2019. A selective fungal transport organ (mycangium) maintains coarse phylogenetic congruence between fungus-farming ambrosia beetles and their symbionts. Proceedings of the Royal Society B: Biological Sciences. 286:2018–2127.

Smith SM, Gomez DF, Beaver RA, Hulcr J, Cognato AI. 2019. Reassessment of the species in the *Euwallacea Fornicatus* (Coleoptera: Curculionidae: Scolytinae) complex after the rediscovery of the "lost" type specimen. Insects 10:2406–2406.

Spahr E, Kasson MT, Kijimoto T. 2020. Micro-computed tomography permits enhanced visualization of mycangia across development and between sexes in *Euwallacea* ambrosia beetles. PLoS ONE 15: e0236653.

Stamatakis A. 2014. RAxML version 8: a tool for phylogenetic analysis and post-analysis of large phylogenies. Bioinformatics 30:1312–1313.

Stouthamer R, Rugman-Jones P, Thu PQ, Eskalen A, Thibault T, Hulcr J, Wang LJ, Jordal BH, Chen CY, Cooperband M, Lin CS, Kamata N, Lu SS, Masuya H, Mendel Z, Rabaglia R, Sanguansub S, Shih HH, Sittichaya W, Zong S. 2017. Tracing the origin of a cryptic invader: phylogeography of the *Euwallacea fornicatus* (Coleoptera: Curculionidae: Scolytinae) species complex. Agricultural and Forest Entomology 19:366–375.

Vega FE, Biedermann PHW. 2020. On interactions, associations, mycetangia, mutualists and symbiotes in insect-fungus symbioses. Fungal Ecology 44: 100909.

White TJ, Bruns T, Lee S, Taylor J. 1990. Amplification and direct sequencing of fungal ribosomal RNA genes for phylogenetics. In: Innis MA, Gelfand DH, Sninsky JJ, White TJ, eds. PCR protocols: a guide to methods and application. San Diego, CA: Academic Press. p. 315–322